



**HAL**  
open science

## Lake Chad sedimentation and environments during the late Miocene and Pliocene: New evidence from mineralogy and chemistry of the Bol core sediments

Abderamane Moussa, Alice Novello, Anne-Elisabeth Lebatard, Alain Decarreau, Claude Fontaine, Doris Barboni, Florence Sylvestre, Didier Bourlès, Christine Paillès, Guillaume Buchet, et al.

### ► To cite this version:

Abderamane Moussa, Alice Novello, Anne-Elisabeth Lebatard, Alain Decarreau, Claude Fontaine, et al.. Lake Chad sedimentation and environments during the late Miocene and Pliocene: New evidence from mineralogy and chemistry of the Bol core sediments. *Journal of African Earth Sciences*, 2016, 118, pp.192-204. 10.1016/j.jafrearsci.2016.02.023 . hal-01716155

**HAL Id: hal-01716155**

**<https://hal.science/hal-01716155v1>**

Submitted on 23 Feb 2018

**HAL** is a multi-disciplinary open access archive for the deposit and dissemination of scientific research documents, whether they are published or not. The documents may come from teaching and research institutions in France or abroad, or from public or private research centers.

L'archive ouverte pluridisciplinaire **HAL**, est destinée au dépôt et à la diffusion de documents scientifiques de niveau recherche, publiés ou non, émanant des établissements d'enseignement et de recherche français ou étrangers, des laboratoires publics ou privés.

# Accepted Manuscript

Lake Chad sedimentation and environments during the late Miocene and Pliocene: new evidence from mineralogy and chemistry of the Bol core sediments

Abderamane Moussa, Alice Novello, Anne-Elisabeth Lebatard, Alain Decarreau, Claude Fontaine, Doris Barboni, Florence Sylvestre, Didier L. Boulès, Christine Paillès, Guillaume Buchet, Philippe Duringer, Jean-François Ghienne, Jean Maley, Jean-Charles Mazur, Claude Roquin, Mathieu Schuster, Patrick Vignaud, Michel Brunet



PII: S1464-343X(16)30078-4

DOI: [10.1016/j.jafrearsci.2016.02.023](https://doi.org/10.1016/j.jafrearsci.2016.02.023)

Reference: AES 2514

To appear in: *Journal of African Earth Sciences*

Received Date: 7 September 2015

Revised Date: 26 February 2016

Accepted Date: 27 February 2016

Please cite this article as: Moussa, A., Novello, A., Lebatard, A.-E., Decarreau, A., Fontaine, C., Barboni, D., Sylvestre, F., Boulès, D.L., Paillès, C., Buchet, G., Duringer, P., Ghienne, J.-F., Maley, J., Mazur, J.-C., Roquin, C., Schuster, M., Vignaud, P., Brunet, M., Lake Chad sedimentation and environments during the late Miocene and Pliocene: new evidence from mineralogy and chemistry of the Bol core sediments, *Journal of African Earth Sciences* (2016), doi: 10.1016/j.jafrearsci.2016.02.023.

This is a PDF file of an unedited manuscript that has been accepted for publication. As a service to our customers we are providing this early version of the manuscript. The manuscript will undergo copyediting, typesetting, and review of the resulting proof before it is published in its final form. Please note that during the production process errors may be discovered which could affect the content, and all legal disclaimers that apply to the journal pertain.

1 **Lake Chad sedimentation and environments during the late Miocene and Pliocene: new**  
2 **evidence from mineralogy and chemistry of the Bol core sediments**

3  
4 Abderamane Moussa<sup>1</sup>, Alice Novello<sup>2,3</sup>, Anne-Elisabeth Lebatard<sup>3</sup>, Alain Decarreau<sup>4</sup>, Claude  
5 Fontaine<sup>4</sup>, Doris Barboni<sup>3</sup>, Florence Sylvestre<sup>3</sup>, Didier L. Bourlès<sup>3</sup>, Christine Paillès<sup>3</sup>,  
6 Guillaume Buchet<sup>3</sup>, Philippe Durringer<sup>5</sup>, Jean-François Ghienne<sup>5</sup>, Jean Maley<sup>6</sup>, Jean-Charles  
7 Mazur<sup>3</sup>, Claude Roquin<sup>5</sup>, Mathieu Schuster<sup>5</sup>, Patrick Vignaud<sup>7</sup>, Michel Brunet<sup>7,8</sup>

8  
9 <sup>1</sup>Département de Paléontologie, Université de N'Djamena, BP 1117, N'Djamena, Chad

10 <sup>2</sup>Evolutionary Studies Institute, University of the Witwatersrand, Johannesburg, South Africa

11 <sup>3</sup>Aix-Marseille Université, CNRS, IRD UMR 34 CEREGE, Technopôle de l'Environnement  
12 Arbois-Méditerranée, BP80, 13545 Aix-en-Provence, France

13 <sup>4</sup>IC2MP, Institut de Chimie des Milieux et Matériaux de Poitiers, UMR 7285 CNRS -  
14 Université de Poitiers, 4 rue Michel Brunet - TSA 51106, 86073 Poitiers Cedex 9, France

15 <sup>5</sup>Institut de Physique du Globe de Strasbourg, UMR7516, CNRS - Université de  
16 Strasbourg/EOST, 1 rue Blessig, 67084 Strasbourg Cedex, France

17 <sup>6</sup>IRD & Département Paléoenvironnements, Institut des Sciences de l'Evolution de  
18 Montpellier, UMR 5554 CNRS, Université de Montpellier II, 34095 Montpellier, Cedex 5,  
19 France

20 <sup>7</sup>iPHEP, Institut de Paléoprimatologie, Paléontologie Humaine : Evolution et  
21 Paléoenvironnements,

22 UMR 7262 CNRS-INEE - Université de Poitiers, 6 rue Michel Brunet, 86073 Poitiers Cedex  
23 9, France

24 <sup>8</sup>Collège de France, Chaire de Paléontologie humaine, 3 Rue d'Ulm 75231 Paris Cedex 05

25  
26  
27  
28  
29  
30  
31 Corresponding author: A.Novello, novelloalice@gmail.com

32 *Present address:* Evolutionary Studies Institute, University of the Witwatersrand,  
33 Johannesburg, South Africa

34

**35 Abstract (164 words)**

36 This study presents mineralogical and geochemical data from a borehole drilled near the  
37 locality of Bol (13°27'N, 14°44'E), in the eastern archipelago of the modern Lake Chad  
38 (Chad). Samples were taken from a ~200 meters long core section forming a unique sub-  
39 continuous record for Central Africa. Among these samples, 35 are dated between 6.4 and 2.3  
40 Ma. Dominant minerals are clays (66% average) mixed with varying amounts of silt and  
41 diatomite. The clay fraction consists of Fe-beidellite (87% average), kaolinite, and traces of  
42 illite. Clay minerals originate from the erosion of the vertisols that surrounded the paleolake  
43 Chad. Sedimentological data indicate that a permanent lake (or recurrent lakes) existed from  
44 6.7 until 2.3 Ma in the vicinity of Bol. By comparison with modern latitudinal distribution of  
45 vertisols in Africa the climate was Sudanian-like. Changes in the sedimentation rate suggest a  
46 succession of wetter and dryer periods during at least six million years in the region during  
47 the critical time period covering the Miocene-Pliocene transition.

48

49 **Key words:** Lake Chad, Miocene-Pliocene, Fe-beidellite, vertisol, sedimentation rate

50

**51 1 Introduction**

52 Lake Chad is a permanent and shallow freshwater body located in the Sahelian domain of  
53 Africa that fringes the southern edge of the Sahara desert (Fig.1). It is today mostly supplied  
54 from its southern watershed by the Chari-Logone rivers system. Lake Chad is a very sensitive  
55 indicator of climate and environment changes in North-Central Africa as illustrated by its  
56 dramatic recent and past shrinkage in area (Maley, 1972, 2010; Maley and Vernet, 2015).  
57 During the 1960's, Lake Chad covered 25000 km<sup>2</sup>. It decreased less than 1500 km<sup>2</sup> during the  
58 1980's (Olivry *et al.*, 1996; UNEP, 2004; Don-Donné Goudoum and Lemoalle, 2014), whereas  
59 during the Holocene, 6000 years ago, it reached >350000 km<sup>2</sup> (Schuster *et al.*, 2005) (Fig.1).

60 The Chad basin is an intracratonic sag basin, whose margins correspond to the maximum  
61 expansion of the lake during the Holocene (Schuster *et al.*, 2005; Leblanc *et al.*, 2006). The  
62 basin basement includes a suite of crystalline rocks related to the Pan-African orogeny (ca.  
63 750-550 Ma), which is directly covered by Cretaceous sandstones (Bessoles and Trompette,  
64 1980). On top of the Cretaceous deposits, it also includes Neogene and quaternary sediments  
65 of about 500 m thick covering an area of about 500 km in diameter (Burke *et al.*, 1976).

66 Scarce sedimentological data coming from petroleum exploration in Niger, Central African  
67 Republic, and Chad (Genik, 1992) give a brief history of the filling of rift basins in Central

68 Africa, which were since completed by significant sedimentological investigations at the  
69 hominin-bearing deposits of northern Chad (Brunet *et al.*, 1995, 2002, 2005). Regarding  
70 southwestern Chad, Genik reports the late Miocene in the Doba and Dosea basins as thick  
71 (200 to 800 m) non-marine sandstones, while Kusnir and Moutaye (1997) described very  
72 briefly the central basin sedimentary series as formed by Cretaceous sandstones followed by a  
73 sandy early Pliocene and a limnic argillaceous middle and late Pliocene. More recently,  
74 Swezey (2009) presented three stratigraphic sections described by Schneider and Wolf  
75 (1992), where the Pliocene sediments are briefly described as mudstones more or less  
76 diatomaceous and gypsiferous. In the northern part of the basin, multiple fossiliferous sediment  
77 series were described (Schuster *et al.*, 2006, 2009) and overall dated between 7.5 and 1.1 Ma  
78 using the  $^{10}\text{Be}/^9\text{Be}$  method (Lebatard *et al.*, 2010). They consist of many sequences of  
79 lacustrine (clays and diatoms), perilacustrine (argillaceous sandstones with root concretions,  
80 rhizoliths and abundant termite nests) (Durringer *et al.*, 2006, 2007), and aeolian deposits,  
81 suggesting successive and repeated wet and dry climatic periods during the Miocene-  
82 Pliocene. Perilacustrine sediments have yielded a quantity of fossil vertebrate remains  
83 including fishes, turtles, crocodiles, birds, and mammals among which two new species of  
84 hominins, so-called *Sahelanthropus tchadensis* and *Australopithecus barhelghazali* (Brunet *et*  
85 *al.*, 1995, 2002, 2005) (Fig.1).

86 The discovery of early hominins in northern Chad has notably reinforced some people's  
87 interest in the region and its environmental past. Indeed, understanding human evolution  
88 implies to capture the environmental context of hominin occurrences in the fossil record, and  
89 to determine the factors that may have influenced their repartition and evolution through time  
90 (e.g. Levin, 2015). Many studies led in northern Chad have thus far focused on documenting  
91 the paleoenvironment at the key moments of hominin occurrences (e.g. Zazzo *et al.*, 2000;  
92 Boisserie *et al.*, 2005; Vignaud *et al.*, 2002; Jacques, 2007; Blondel *et al.*, 2010; Otero *et al.*,  
93 2010; Pinton *et al.*, 2010; Lee-Thorp *et al.*, 2012; LeFur *et al.*, 2009, 2014) without really  
94 contextualizing their results in the broader background of paleoenvironmental and  
95 paleoclimatic changes in North-Central Africa during the Neogene. The same studies  
96 provided evidence of mosaic environments including forest patches, woodland, and  
97 grasslands in close relationship with aquatic areas at the time of *S. tchadensis* occurrence (ca  
98 7 Ma) (Boisserie *et al.*, 2005; Vignaud *et al.*, 2002; Jacques, 2007; Blondel *et al.*, 2010; Otero  
99 *et al.*, 2010; Pinton *et al.*, 2010; LeFur *et al.*, 2009, 2014), and described the environment of  
100 *A. barhelghazali* as more open and dominated by C<sub>4</sub> vegetation (Zazzo *et al.*, 2000; Lee-

101 Thorp *et al.*, 2012). A few studies, conversely, have addressed the questions of the evolution  
102 of paleoenvironments in Chad by comparing data on a deep-time scale from the end of the  
103 late Miocene to the late Pliocene (Otero *et al.*, 2011; Novello *et al.*, 2015a, 2015b). Oxygen  
104 isotope analyses conducted on fish teeth suggest a trend toward increased regional aridity  
105 between 7 and 3 Ma in northern Chad, including a more abrupt shift at the Miocene-Pliocene  
106 transition during the time spanning across the Messinian salinity crisis in the Mediterranean  
107 region (Otero *et al.*, 2011). A multi-proxy approach was recently performed on a new  
108 sedimentary record related to a core drilled close to the locality of Bol, which is located at the  
109 limit between the northern and southern parts of the Lake Chad basin, in the northeast  
110 archipelago of the current Lake Chad (Fig.1). This sub-continuous sedimentary archive was  
111 dated between 6.3 and 2.3 Ma using the  $^{10}\text{Be}/^9\text{Be}$  method (Novello *et al.*, 2015a, 2015b), and  
112 it therefore gives the opportunity to document the paleoenvironment and paleoclimate  
113 evolution of this part of the Lake Chad basin on a deeper time scale than the sporadic  
114 Miocene and Pliocene series of northern Chad. The diatom assemblages of this record reveal  
115 the existence (even interrupted) of lacustrine conditions at  $13^\circ\text{N}$  in Chad since at least  $4.7\pm 0.1$   
116 Ma, while phytoliths and pollen support the presence of grass-dominated environments in the  
117 area of Bol and probably further south in the southern part of the basin during all the Pliocene  
118 (Novello *et al.*, 2015a, 2015b). A decrease of lacustrine conditions was suggested between  
119  $3.6\pm 0.1$  Ma to  $2.7\pm 0.1$  in the vicinity of Bol and deduced from the scarcity of diatom remains  
120 and the increase of marsh indicator phytoliths in the sequence (Novello *et al.*, 2015a, 2015b).  
121 This last result corroborates three sudden aridity events recorded successively in north-  
122 western Africa at about 3.5, 3.2, and 2.8 Ma (Leroy and Dupont, 1994, 1997) and suggests  
123 that dry conditions were extended all over North-West and Central Africa between  $\sim 3.6$  and  
124 2.7 Ma.

125 Here, we present the results obtained after a series of mineralogy analyses performed on the  
126 Bol core sequence (Moussa, 2010; Moussa *et al.*, 2013). This study is a valuable complement  
127 to the previous micro-biological data published in Novello *et al.* (2015a, 2015b), by providing  
128 new clues about the Lake Chad history, and about the paleoenvironment and paleoclimate in  
129 Central Africa from about 6 Ma. It also permits to recall the information already yielded in  
130 Novello *et al.* and to compare all the different types of data produced in order to enhance the  
131 discussions and paleoenvironmental interpretations.

132

## 133 2 Material

134 The samples studied are all cuttings, associated with a 673 m long hydrogeological core  
135 drilled in 1973 by the “Bureau de Recherches Géologiques et Minières” (BRGM, France) on  
136 the northeastern shore of Lake Chad, near the locality of Bol (Fig.1) (13°27’N, 14°44’E). The  
137 core reached the basement (Precambrian metamorphic rocks: gneiss, leptynite) at 673 m depth  
138 (Fig.2a). Cuttings and some core sections have only been preserved from between 70 and 300  
139 m depth since the drilling. Below that, only the lithological log description of the core is still  
140 available. According to original data producing during the coring, the core can be divided into  
141 three major segments from the top to the bottom, which reflect dominant lithology (Fig.2a):

- 142 - From 0 to 71.5 m: eolian sands;
- 143 - From 71.5 to 330 m: pelites more or less mixed with lacustrine diatomites;
- 144 - From 330 to 673 m: silt/sand and clay alternation.

145 The eolian sand formation is related to Kanem dunes deposited during the Last Glacial  
146 Maximum (Servant, 1983; Maley, 2010). Some pelitic samples, located between 71.5 m and  
147 297 m, were dated using the  $^{10}\text{Be}/^9\text{Be}$  (Fig.2, Table S1) (Novello et al., 2015a, 2015b). These  
148 sediments were deposited during the late Miocene and the Pliocene. By comparison with  
149 sediments described in the northern part of the Chad basin (Vignaud et al., 2002; Schuster  
150 2002, Schuster et al., 2005; Düringer et al., 2006), the fine sands and clays occurring between  
151 330 m and 580 m can be attributed to the late Miocene. The basal coarse sands may be  
152 deposited from Eocene to Miocene (Servant-Vildary, 1978; Servant 1983).

153 This study focuses on the second core segment (71.5-297.2 m), which is the only sampled part  
154 of the core still available. The samples studied were taken in the core to about every 2 meters  
155 from 71.5 m to 170 m and then every 6 meters from 170 m to 297.2 m (Fig.2, Table S1). The  
156 micro-biological remains (diatoms, phytoliths, and pollen) of these samples were previously  
157 studied (Novello et al., 2015a, 2015b).

158

## 159 3 Methods

160 The continuous lithology of the core (Fig.2b) was reconstructed using the core lithological log  
161 description and our direct observations of the samples. All of the 126 available samples were  
162 examined using binocular glasses and smear slides. Samples mostly consist of angular core  
163 fragments, but also in rare core sections (9 cm of diameter and 5-7 cm of height). The  
164 mineralogy of 64 samples was semi-quantified using powder X-Ray Diffraction (XRD), and  
165 then ten samples, regularly distributed along the core and previously dated (Novello et al.  
166 2015a, 2015b) (except sample 01d), were studied in details by XRD and by chemical



167 analyses. XRD patterns were obtained with a Philips X'Pert PRO equipped with a Ni-filtered  
168 CuK $\alpha$  radiation generated at 40 kV and 40 mV. A  $1/4$   $2\theta$  anti-divergence slit and a  $1/2$   $2\theta$   
169 anti-diffusion slit were used, step size is 0.017 and step time is 30 s. Scans were taken  
170 between 2.5 and 65° for randomly oriented powder. The XRD patterns were obtained from  
171 powders and oriented preparations of Na, K and, Ca-saturated samples in the air-dried state,  
172 after ethylene glycol solvation, hydrazine solvation, and heating (350°C, 4 h). Semi-  
173 quantification of minerals amounts was obtained using the relative areas of the major peaks  
174 on powder patterns. Local chemical analyses of bulk samples were performed on core  
175 fragments (from 0.5 to 1 cm in diameter) with a JEOL JSM-5600LV scanning electron  
176 microscope (SEM) equipped with an EDX system (Bruker AXS Microanalysis). The clay  
177 fraction ( $<2\mu\text{m}$ ) of the ten samples was analyzed for major elements and trace elements at  
178 Nancy SARM, using the ICP-MS method (Carignan *et al.* 2001).

179

## 180 **4 Results**

### 181 *4.1. Lithological description*

182 The studied samples range from claystones to siltstones. These are laminated but not varved,  
183 which gives a succession of millimetric to centimetric lamina of clays, silts/sands, and  
184 diatomites (Fig.2b). The major component is grey to light green clays. These clays occur as  
185 pelites, which are more or less mixed with silts/sands and/or diatomites. White diatomites are  
186 generally mixed with clays and/or silts/sands.

187 All samples consist of fine grained clayey sediments. The largest grains observed consist only  
188 in quartz grains (coarse sand) of 1 to 2 mm of diameter. Most of quartz grains, conversely, are  
189 between 200 and 500  $\mu\text{m}$  and with a river transported grain morphology. Few amounts of  
190 typical aeolian quartz grains are also observed and they are always mixed with other quartz  
191 grains in some samples (2f, 8j, 25a, and 17h notably) (Table S1). Ovoid pellets of indurated  
192 mud, from 1 mm up to 1 cm, occurred in samples 21j and 35e (Table S1).

193 Laminated structures are observed in the samples studied all along the core. Most often  
194 millimetric lamina of clays alternate with some diatomites or silt/sand lamina. Silt/sand layers  
195 are never more than 5 mm thick. In few samples (18h, 12b, and 9e) (Table S1) few  
196 millimeters thick layers of diatomite and clays alternate.

197 Between 90.8 m to 92.3 m, and 100.3 to 103.7 m, all samples (5a to 5m, and 7f to 8g) (Fig.2b)  
198 include tubular holes of several centimeters long and millimetric in diameter cross the



199 sediments. These holes are coated by brown to red very thin deposits of amorphous iron oxy-  
200 hydroxides. These features are similar to rizoliths observed in modern soils.

201 In the available samples no sedimentary features like cross bedding, mud-cracks, and  
202 erosional surface are observed.

203

#### 204 4.2. Sample mineralogy

##### 205 4.2.1. Recurrent minerals

206 According to powder XRD data of the whole rock samples (Fig.3), the main and recurrent  
207 occurring minerals are smectite (001 reflection at 15.3 Å), kaolinite (001 reflection at 7.2 Å),  
208 illite (001 reflection at 10 Å), quartz (main reflection at 3.34 Å), K-feldspars (main reflection  
209 at 3.24 Å), and anatase (main reflection at 3.52 Å). The relative amounts of these minerals  
210 were semi-quantified (Fig.4). Clays are the most important minerals all along the core. Their  
211 relative abundance ranges from 50 to 85 %, with a mean value of 66%. Quartz is the second  
212 mineral represented, ranging from 6 and 70 % (mean value of 27%), while K-feldspars and  
213 anatase are always detected in low amounts (mean values close to 4 and 5 %, respectively).  
214 The whole mineralogy reflects the relative amounts of the silt and sand fractions (quartz, k-  
215 feldspar, and anatase) in sediments dominated by a clay fraction. XRD diagrams of ovoid  
216 pellets of indurated mud in samples 21j and 35e are similar to the ones of the surrounding  
217 pelites.

218

##### 219 4.2.2. Sporadic minerals

220 Opale CT. Biogenic silica is generally made of opal-A, which has a disordered, nearly  
221 amorphous structure. It exhibits only a broad band between 19 and 25 °2θ on XRD patterns  
222 (DeMaster, 2003), which is overlapped by the dissymmetric (02-11) reflection of clay  
223 minerals. Therefore it was not possible to detect and quantify the amounts of opal-A resulting  
224 from the occurrence of diatoms and phytoliths in sediments (Novello et al, 2015a, 2015b). In  
225 the lower part of the core (samples 30j to 35e, from 251 m to 297 m depth), opal- CT was  
226 detected (major peak at 4.03 Å) (Fig.3). According to XRD data, the amounts of opal-CT are  
227 ranging between 20 and 40%. Opal-CT is a well-known product of the early diagenesis of  
228 opal-A (DeMaster, 2003). The biogenic silica of diatoms and phytoliths was transformed in  
229 opal-CT by diagenetic evolution of the deeper samples of the core.

230 Gypsum (mean peak at 7.59 Å) was detected as traces in most samples but in large quantities  
231 in samples 7f, 8a, 8e, 8o, 15h, and 21a-e (Table S1). In these samples, gypsum crystals occur  
232 as millimetric elongated laths. This crystal morphology suggests a diagenetic origin for  
233 gypsum.

234 Calcite and dolomite. Carbonates were rarely detected and in very low amounts (samples 1a-  
235 1d, 11d, 20b, 22n, and 30j, Table S1), except in sample 6a (10 % of calcite and 5% of  
236 dolomite). No shell fragments were observed.

237 Apatite. Apatite occurs as minor component in samples 5g, 6d-h, 9c, 10b, 16i, 17h, and 21j  
238 (Table S1). Apatite source is likely to be related to vertebrate fossil fragments such as fish-  
239 bones.

240 Jarosite (mean peak at 3.07 Å) was detected only in sample 29a (Table S1). Jarosite is a basic  
241 hydrous sulfate of iron and potassium ( $\text{KFe}^{3+}_3(\text{OH})_6(\text{SO}_4)_2$ ) occurring in sulfate rich  
242 environments, most often resulting from the oxidation of pyrite in acidic environments  
243 (Stoffregen et al., 2000). Here it is more likely that jarosite has a diagenetic origin.

244

#### 245 4.3. Detailed studies of clay minerals

##### 246 4.3.1. Relative amounts of clays

247 Clay minerals of samples were carefully studied using the <2 µm fraction. (Fig.5). Smectite,  
248 with a mean value of 87%, is the main clay occurring in the <2 µm fraction all along the core.  
249 The (001) peak of smectite is especially very broad in the samples having the lowest amounts  
250 of this mineral. This feature is due to a very low amount of stacked layers (about 2 layers) of  
251 smectite, which makes its quantification difficult and possibly underestimated. Kaolinite is  
252 the second clay of the <2 µm fraction, with a mean value of 12%. Illite is a minor component  
253 but it is always present in detectable amounts while quartz always occurs in very low  
254 amounts.

255 The clay mineralogy appears quite constant all along the core, with a light increase of  
256 smectite at the top of the core.

257

##### 258 4.3.2. Detailed studies of ten selected samples

#### 259 XRD

260 The (001) reflection located at 15.5 Å in air dry condition shifted to 17.8 Å after ethylene-  
261 glycol treatment, and fell down to 10.0 Å after heating at 350°C (Fig.6). This behavior is  
262 typical of a smectite without interstratification and excludes the occurrence of chlorite  
263 (Brindley and Brown, 1980). A (001) reflection at 15.5 Å in air dry condition indicates the  
264 occurrence of two water molecules in the interlayer of the smectite, and Ca as the main  
265 exchangeable cation. The (06-33) reflection of the smectite ranges from 1.50 to 1.51 Å, which  
266 is characteristic of a dioctahedral layer (Brindley and Brown, 1980). After the Hofmann-  
267 Klemen test (Brindley and Brown, 1980), the (001) reflection of the smectite is at 18 Å. This  
268 feature indicates that its layer charge originates, at least partly, from a tetrahedral charge,  
269 which is characteristic of beidellite-like smectite. After successive saturations of samples by  
270 Ca, K, and then by Ca and ethylene-glycol treatments, the (001) reflection of the smectite is at  
271 18 Å. This behavior is typical of low to medium charge smectite layers (Brindley and Brown,  
272 1980).

273 After hydrazine saturation, the (001) reflection of kaolinite partly remains at 7.14 Å while  
274 another part shifts to 10.4 Å (Fig.7). This indicates a mixture of ordered and disordered  
275 kaolinite crystals. The amount of disordered kaolinite crystals ranges from 41 to 85 % (Table  
276 1).

277 No difference was found between the XRD patterns of clays in pellets and surrounding pelite  
278 for samples 21j and 35e (Table S1). Pellets are due to a reworking of pelite (rip-up clasts).

279

### 280 Chemical analyses

281 Two sets of data were collected: bulk analyses of the <2 µm fraction of samples (Table 2) and  
282 local analyses using a scanning electronic microprobe (Table 3). Both data gave consistent  
283 results. The mineralogy of the <2 µm fraction consists of smectite, kaolinite, minor illite, and  
284 quartz. The variations in SiO<sub>2</sub> contents are linked to the amounts of quartz and kaolinite.  
285 Because natural kaolinite crystals contain low amounts of Fe<sub>2</sub>O<sub>3</sub> (Mestdagh et al, 1980) and  
286 illite is a minor component, the major part of Fe<sub>2</sub>O<sub>3</sub> is therefore represented by smectite.  
287 Between 10 and 20% of the Al<sub>2</sub>O<sub>3</sub> amounts come from kaolinite. The MgO contents are low  
288 and essentially related to smectite. As illite is a minor component of samples, a part of K<sub>2</sub>O is  
289 associated with the smectite phase. According to these data, the smectite present in all the  
290 samples has a chemistry characterized by large amounts of Al and Fe, and by low Mg and K  
291 contents. It was however not possible to establish the structural formula of the smectite  
292 because of the complex mineralogy of the samples.

293 The chemistry of the <2  $\mu\text{m}$  fraction in ovoid pellets (samples 21j and 35e) (Table S1) is very  
294 close to that present in the surrounding pelite (Table 2). The higher amount of  $\text{SiO}_2$  in sample  
295 35e° is probably due to its higher quartz composition.

296 SEM-EDX measurements did not allow obtaining the chemistry of isolated smectite particles.  
297 At the micron size scale, smectite, kaolinite, and quartz particles are intimately joined. Al, Fe,  
298 Mg, and K ratios measured by SEM-EDX are similar to those obtained by bulk chemical  
299 analysis (Table 3).

300 Rare earth elements (REE) diagrams of the <2  $\mu\text{m}$  fraction (Fig.8a) are very similar between  
301 the ten samples. Similarities are also observed between all the samples for the extended  
302 diagrams of trace elements (Fig.8b).

303

#### 304 The smectite component

305 Smectite is the main mineral of the clay fraction (mean value 87 %) and the main component  
306 of all the samples (main value 57%). Among the various kinds of smectite minerals existing,  
307 the smectite occurring in the Bol sediments possesses a dioctahedral feature and a tetrahedral  
308 charge, in addition to contain large amounts of iron. These are all characteristics of a Fe-  
309 beidellite (smectite) (Brindley and Brown, 1980).

310

## 311 **5 Discussion**

### 312 *5.1. Source of the deposits*

313 The recurrent occurrence of freshwater organism remains (diatoms, sponges), and notably the  
314 dominant freshwater diatom species *Aulacoseira granulata* (Novello et al., 2015a, 2015b)  
315 indisputably suggests the existence of true lacustrine environments at Bol during the  
316 Miocene-Pliocene. Quartz grain morphology indicates that the major inputs of quartz to the  
317 lake originated from fluvial transport while a few parts originated from aeolian transport  
318 only. Comparably, pollen spectra of Lake Chad also indicate significant fluvial  
319 contributions to the lake during the Holocene (Maley, 1972, 1981) and still today (Maley,  
320 2010).

321 The dominance of finely laminated clays among the sediments indicates deposition by  
322 settling. REE diagrams of the clay fraction (Fig.8a) are similar to diagrams of detrital  
323 sediments derived from post archean continental crust, with notably similar  $\text{La}_N/\text{Yb}_N$  and  
324  $\text{Eu}/\text{Eu}^{**}$  values all along the core (McLennan, 1989). The relatively high values of  $\text{La}_N/\text{Yb}_N$

325 are typical of claystones (McLennan, 1989). The similarity of REE and extended trace  
326 elements diagrams (Fig.8b) between all the samples suggests that the same basement rock was  
327 eroded and then deposited to feature in the Bol sequence. Trace element diagrams strongly  
328 suggest a detrital origin for the clay minerals and notably the Fe-beidellite. Authigenic  
329 pelloidal nontronites are not observed in the Bol sediments while they are present in modern  
330 lake Chad sediments sampled in the Chari Logone delta (Pedro *et al.*, 1978). This last result  
331 coupled with the lack of cross beddings (at the scale of the core) and the absence of coarse  
332 sand deposits indicate that Bol was far from any major river delta during the total period of  
333 sediments' deposition. The changing proportions between pelite, silt-sand, and diatomite  
334 result principally from the variation in time of the rivers discharges in the Chad basin.

335 Today, the detrital sediments deposited in the Lake Chad basin are essentially transported by  
336 the Chari-Logone system (Fig.1) and mostly originate from the erosion of the southern part of  
337 the watershed, which is characterized by important reliefs (the Adamawa mounts, ~1900 m  
338 above the sea level) and by mean annual rainfall of 1200 mm (Olivry *et al.*, 1996). This part  
339 of the drainage basin is currently covered by ferralitic and tropical ferruginous soils, in which  
340 kaolinite is the dominant clay (Gac 1980). The suspended clays in the Chari river, near Lake  
341 Chad, are indeed dominated by kaolinite. A smaller part of the current sediments deposited in  
342 the Chad basin also comes from the erosion of the lowlands located in the north of the Chari-  
343 Logone watershed (Gac, 1980), which are essentially covered by vertisols dominated by  
344 smectite (Fe-beidellite) clay minerals (Paquet, 1970). As a result, the current ratio  
345 kaolinite/illite/smectite in the modern Lake Chad sediments is close to 63/19/18 %  
346 (Carmouze, 1976; Carmouze *et al.*, 1977; Gac, 1980; Gac *et al.*, 1977). In the Bol sediments,  
347 the smectite is conversely largely dominant, with a ratio kaolinite/illite/smectite equivalent to  
348 12/1/87 %. Paquet (1970) observed that kaolinite has a higher crystallinity in ferralitic soils of  
349 Central Africa than in vertisols in general. In the Bol sediments, badly crystallized  
350 (disordered) kaolinites occur in higher abundance than well crystallized kaolinites (Table 1).  
351 This last result suggests a partial sedimentary contribution from ferralitic soils of the southern  
352 part of the Chad watershed during the Miocene-Pliocene, while most of the contribution was  
353 originated from the erosion of vertisols of the lowlands. A higher contribution from the  
354 southern highlands than today was suggested by Novello *et al.* (2015a, 2015b) as an  
355 interpretation of the significant percentage of Afromontane pollen at  $4.2 \pm 0.1$  Ma and the  
356 unexpected occurrence of C<sub>3</sub> grass indicator phytoliths in the Bol sediments. Yet, none of the

357 mineralogy data support a trend towards an increase of highlands contribution during the  
358 Miocene-Pliocene.

### 359 5.2. Lake morphology and dynamics

360 Similarities between ovoid pellets of mud and their surrounding matrix at  $3.7\pm 0.1$  Ma and  
361  $6.4\pm 0.1$  Ma (samples 21j and 35e) suggest a clay rip-up clasts origin. These pellets may have  
362 been produced after the sediments eroded and deposited in the lake, probably in a context of  
363 lake regression. Hence, this would suppose rapid changes of the lake water levels at Bol  
364 during the end of the late Miocene and during the mid-Pliocene. Moreover, it is most likely  
365 that Bol was in the nearshore zone of the lake during these periods which would explain it  
366 recording such abrupt variations of the lake level. The closeness of Bol to the lake and the low  
367 lake level hypotheses during the end of the late Miocene is consistent with the phytolith  
368 assemblage observed at  $5.5\pm 0.1$  Ma (sample 30j), which includes about 13% of phytoliths  
369 indicators of palms (terrestrial obligate plants), against a mere <2-5% in the other samples of  
370 the core (Novello *et al.*, 2015a, 2015b). Later on between ~2.6 and 2.4 Ma, rhizoliths are  
371 observed, suggesting again that Bol was close to the lake's shore. Given the lack of true  
372 pedogenesis features in the samples, however, it is likely that these rhizoliths were associated  
373 with aquatic plants in a shallow water environment (marshy vegetation).

374 Hydrous sodium silicates including magadiite, kenyaite, and zeolites were described in the  
375 N'Guigmi interdunal depressions of Lake Chad (Sebag *et al.*, 2001). These sodium silicates  
376 were formed from brines during the Holocene and indicate a strong evaporation rate of Lake  
377 Chad during the last 10,000 years. No such silicates were observed in the Bol samples,  
378 suggesting therefore the lack of complete, or else near complete, evaporation at Bol. Bio-  
379 silica remains (opal-A), including lacustrine indicators (diatoms and sponge spicules), were  
380 not observed in the deeper part of the core ( $<5.5\pm 0.1$  Ma) (Novello *et al.*, 2015a, 2015b),  
381 while opal-CT was detected (this study). The siliceous remains initially made of opal-A may  
382 have been transformed into opal-CT by diagenesis, preventing their direct recognition by the  
383 diatom and phytolith specialists. From 6.4 to 2.3 Ma, therefore, water seems to have been  
384 always present at Bol even during periods of the lowest lake levels which favored marshy  
385 vegetation (Novello *et al.*, 2015a, 2015b).

386 The relative amounts of clays, silt/sands, and diatomites in the Bol sediments can be  
387 interpreted as indicating changes in the runoff intensity during Miocene-Pliocene. During a  
388 full year, the amount of detrital sediments transported to the current Lake Chad by the Chari-



389 Logone system is positively correlated with the intensity of rainfall in the drainage basin  
390 (Gac, 1980). We assumed that such a correlation had already existed during the Miocene-  
391 Pliocene and hypothesized the following scenario: during rainy periods, a severe erosion of  
392 the river watershed may have occurred, leading to the transport and then deposition of clays  
393 and silt-sands, mixed with diatomites; during periods of weak erosion of the river watershed  
394 (and then more likely dryer conditions in the drainage basin), which are also correlated with  
395 lower lake levels, diatomites may have been deposited (Lemoalle, 1978). This last hypothesis  
396 refers to the observation of significant bloomings of diatoms during periods of low Lake Chad  
397 levels and increasing aridity in the basin during the 1970's (Lemoalle, 1978).

398 The sedimentation rate at Bol was not strictly uniform between the upper Miocene and the  
399 lower Pleistocene. Mean sedimentation rates were calculated using the thickness of sediments  
400 between two dated samples (Fig.2b). A succession of low and high sedimentation rates  
401 occurred during the Miocene-Pliocene (Fig.9). High sedimentation rates are observed for  
402 three distinct periods: 5.6-4.7 Ma, 3.7-3.5 Ma, and 4.3-4.2 Ma (with a lower intensity).  
403 Lacustrine sediments described at the fossiliferous localities of northern Chad (Kollé, Koro  
404 Toro, and Kossom Bougoundi, 16-17°N) (Fig.1) indicate at least three transgressive events of  
405 the lake up to the northern part of the basin during the Pliocene. These events were dated to  
406  $5.4 \pm 0.6$ ,  $4.0 \pm 0.1$ , and  $3.7 \pm 0.1$  Ma using the  $^{10}\text{Be}/^9\text{Be}$  method (Schuster *et al.*, 2009;  
407 Lebatard *et al.*, 2010). The first and last events at  $5.4 \pm 0.6$  and  $3.7 \pm 0.1$  Ma are concomitant  
408 with periods of high sedimentation rate at Bol, and would therefore be associated with an  
409 increase of humid conditions in the drainage basin during these ages. The less remarkable yet  
410 also high sedimentation rate observed between 4.3-4.2 Ma may be correlated to the  
411 transgressive event recorded at  $4.0 \pm 0.1$  Ma in northern Chad depending on whether or not the  
412 uncertainty on the absolute ages is taken into account. According to Schneider and Wolf's  
413 data (1992), Swezey (2009) described the lithology of three wells drilled in the Kanem region  
414 (Fig.1), which each represents a thick section >200 m of mudstones, diatomaceous, and  
415 gypsiferous mudstones. The same author attributed these wells to the Pliocene, while  
416 Schneider (1989) identified the mudstone sections as being partly late Miocene and Pliocene.  
417 It is noteworthy that a great similarity exists between the stratigraphic lithology of the Kanem  
418 wells (made of alternating mudstones and diatomitic layers with dominant mudstones) and the  
419 lithology of the Bol core. All the northern Chad deposits and cores provide evidence that Lake  
420 Chad (or a system of multiple lakes) extended as far as 16°N during the Miocene-Pliocene.  
421 Such an expansion was also observed for the Holocene, a period during which Lake Chad



422 reached its maximum commonly described as Megalake (Schuster *et al.*, 2005; Leblanc *et al.*,  
423 2006; Maley, 2010). In contrast, today Lake Chad is restricted below 14°N.

#### 424 5.3.A lake older than previously thought

425 The  $^{10}\text{Be}/^9\text{Be}$  dating method provided ages ranging from  $6.4 \pm 0.1$  Ma for the sample at 297 m  
426 to  $2.4 \pm 0.1$  Ma for the sample at 90.8 m (Fig.2). Novello *et al.* (2015a, 2015b) used a model to  
427 re-estimate a few  $^{10}\text{Be}/^9\text{Be}$  ages which were chronologically inconsistent. Sediments between  
428 297 m and 330 m are dominated by lacustrine clay sediments which are similar to those  
429 occurring in the upper part of the core. We assume the age model used by Novello *et al.*  
430 (2015a, 2015b) to be totally relevant for estimating the age of the sediment sample located at  
431 330 m. According to this model, the age of the 330 m-deep sample is  $6.7 \pm 0.1$  Ma (Fig.2).  
432 Hence a lake (or successive lakes) existed at Bol as early as  $6.7 \pm 0.1$  Ma ago, which is about  
433 300 ka older than the age published in Novello *et al.* (2015a, 2015b)..

434

#### 435 5.4. Paleoenvironment and paleoclimatology

436 As mentioned above (see section 5.1. in the Discussion), the dominant clay mineral occurring  
437 in the Bol sediments is a smectite, and more precisely a Fe-beidellite, originated from the  
438 alteration of lowlands surrounding the lake and/or present further south in the drainage basin.  
439 This type of beidellite has been described in modern vertisols of many countries (Wilson,  
440 2013): Turkey (Özkan and Ross 1979; Güzl and Wilson, 1981), Morocco (Badraoui and  
441 Bloom, 1990), Sudan (Wilson and Mitchell, 1979), Sardinia (Righi *et al.* 1998), and India  
442 (Math and Murphy, 1994). Paquet (1967, 1970) also described Fe-beidellite crystals with a  
443 similar chemistry in modern vertisols of Central Africa, and notably in the Chad basin.  
444 Vertisols, often named dark clay soils, are today distributed between 45°N and 45 °S of  
445 latitude (excluding the desert area) under climates displaying mean annual precipitation of  
446 500 to 1000 mm and a dry season length of 4 to 8 months over the year (Buol *et al.*, 2011).  
447 The most extensive areas of vertisols of Africa are located in lowlands of Sudan, Egypt,  
448 Ethiopia, and Chad (Buol *et al.*, 2011). In Chad, these areas are represented by the current  
449 Sudanian phytogeographical domain (White, 1983), which is dominated by mixed and open  
450 grassland vegetation. Thus, the dominance of Fe-beidellite in the clay mineral assemblages of  
451 Bol supports Sudanian-like environmental conditions in the southern part of the basin during  
452 the Miocene-Pliocene. This conclusion is consistent with phytolith and pollen remains of the  
453 Bol core (Novello *et al.*, 2015a, 2015b), which indicate humid grass-dominated vegetation in  
454 the surroundings of Bol and/or in the southern part of the basin during the Pliocene. It is also

455 in agreement with vegetation simulations of tropical savanna in the southern Chadian basin at  
456 ~3.6-2.6 Ma (Salzmann *et al.*, 2008; Contoux *et al.*, 2013). Today, Bol area is located in a  
457 drier area, the Sahelian phytogeographical domain (White, 1983), where mean annual rainfall  
458 is <500mm/year and dry season lasts 9 to 11 months.

459 Sedimentation rates are not uniform between the late Miocene and the early Pleistocene. If  
460 one considers detrital sedimentation and rainfall intensity as positively correlated (see section  
461 5.2. in the Discussion), high sedimentation rates recorded in between 5.6-4.7 Ma, 3.7-3.5 Ma,  
462 and to a lesser extent between 4.3-4.2 Ma may result from an increase of the soil erosion in  
463 the drainage basin. Intense soil erosion could be observed in a context of annual rainfall  
464 increase and/or a more pronounced monsoon period. The opposite argument would assume  
465 the low sedimentation rate observed between 3.4-2.7 Ma as a decrease of annual rainfall  
466 and/or an increase of the dry season length in the drainage basin. These hypotheses are in  
467 agreement with phytolith and diatom data, which suggest a decrease of lacustrine conditions  
468 at Bol after ~3.6 Ma and until 2.7 Ma, coupled with drier conditions in the surrounding and/or  
469 in the drainage basin (Novello *et al.*, 2015a, 2015b).

470 Both northern Chad and Bol sedimentary deposits indicate a succession of wetter and drier  
471 conditions in Central Africa during the Miocene-Pliocene, although climatic conditions were  
472 generally more humid over the basin than today. The alternating of drier and wetter periods in  
473 the series is observed from at least ~8 Ma in the northern part of the basin (16°N), and from at  
474 least ~6 Ma in the southern part of the basin (13°N). Humid and arid phases were also  
475 recorded in central Chad during the late Pleistocene (Gasse, 2000; Maley, 2010). The long-  
476 term variability of central African climate is probably related to that recorded in West Africa  
477 during the Neogene and associated with changes in the precessional cyclicity of the Earth's  
478 orbit (deMenocal, 2004). The existence of more humid conditions over the basin during the  
479 Miocene-Pliocene would suggest a more northerly position of the ITCZ (Inter-Tropical  
480 Convergence Zone) during the summer monsoon rainfall (Contoux *et al.*, 2013; Novello *et al.*,  
481 2015a, 2015b). According to Sepulchre *et al.* (2006), the massive uplift occurring in East  
482 Africa after 8 Ma may have impacted moisture circulation between East and Central Africa.  
483 Oxygen isotope analyses performed on fish tooth remains from northern Chad (Otero *et al.*,  
484 2011) indicate a trend towards aridification over the Chadian basin during the Pliocene, which  
485 could illustrate the eastern uplift hypothesis. The Bol data, which suggest drier conditions in  
486 the surroundings and/or in the drainage basin during the late Pliocene (~3.4-2.7 Ma) (Novello

487 et *al.*, 2015a, 2015b; this study), may also have been indirectly affected by the eastern uplift  
488 event. Other factors such as warm temperatures, significantly elevated  $p\text{CO}_2$  compared to  
489 present times, and/or modifications in the ocean circulation and trade wind resulting from the  
490 Northern Hemisphere Glaciation (Feakins and deMenocal, 2010; Pagani et al., 2010;  
491 Salzmann, 2011; Levin, 2015) could have played a role in the aridification of  
492 paleoenvironments in Central Africa during the Pliocene. Yet, the impact of these multiple  
493 changes is still difficult to assess and quantify at the mere scale of the Chad basin.

494

#### 495 **Acknowledgements**

496 This work represents one part of Moussa's PhD work conducted at the Universities of  
497 Strasbourg and Poitiers. We thank the Chadian Authorities (Ministère de l'Éducation  
498 Nationale de l'Enseignement Supérieur et de la Recherche, University of Ndjamená, Centre  
499 National d'Appui à la Recherche), the Ministère Français de l'Enseignement Supérieur et de la  
500 Recherche (UFR SFA, University of Poitiers, INEE/CNRS, ANR, Project ANR-09-BLAN-  
501 0238, PI's M. Brunet), and the Ministère Français des Affaires Étrangères (DCSUR Paris and  
502 French Embassy in Ndjamená, Chad; FSP, Project no. 2005-54 of the Franco-Chadian  
503 cooperation) for financial support and permissions to conduct research in Chad. M. Arnold,  
504 G. Aumaître and K. Keddadouche are thanked for their valuable assistance in  $^{10}\text{Be}$   
505 measurements at the ASTER AMS national facility (CEREGE, Aix-en-Provence) which is  
506 supported by the INSU/CNRS, the ANR through the "Projets thématiques d'excellence"  
507 program for the "Équipements d'excellence" ASTER-CEREGE action, IRD and CEA. We  
508 thank the IC2MP laboratory for the financial support for the XRD and SEM analyses. We are  
509 grateful to O. Otero for her detailed comments on this manuscript.

#### 510 **References**

511 Badraoui, M., Bloom, P.R., 1990. Iron high charge beidellite in vertisols and mollisols of the  
512 High Chaouia region of Morocco. *Soil Science Society of American Journal* 54, 267-274.

513

514 Bessoles, B., Trompette, R., 1980. Géologie de l'Afrique. La chaîne panafricaine « zone  
515 mobile de l'Afrique Centrale (partie sud) et zone mobile soudanaise ». Mémoires du BRGM  
516 (Bureau de Recherches Géologiques et Minières), Paris, 375 p.

517

518 Blondel, C., Merceron, G., Andossa, L., Mackaye, H.T., Vignaud, P., Brunet, M., 2010.  
519 Dental mesowear analysis of the late Miocene Bovidae from Toros-Menalla (Chad) and early

- 520 hominid habitats in Central Africa. *Palaeogeography, Palaeoclimatology, Palaeoecology* 292,  
521 184-191.
- 522
- 523 Boisserie, J.-R., Zazzo, A., Merceron, G., Blondel, C., Vignaud, P., Likius, A., Mackaye,  
524 H.T., Brunet, M., 2005. Diets of modern and late Miocene hippopotamids: Evidence from  
525 carbon isotope composition and micro-wear of tooth enamel. *Palaeogeography,*  
526 *Palaeoclimatology, Palaeoecology* 221, 153-174.
- 527
- 528 Brindley, G.W., Brown, G., 1980. *Crystal Structures of Clay Minerals and Their X-ray*  
529 *Identification*. Mineralogical Society, London, 495 p.
- 530
- 531 Brunet, M., Guy, F., Pilbeam, D., Mackaye, H.T., Likius, A., Ahounta, D., Beauvilain, A.,  
532 Blondel, C., Bocherens, H., Boisserie J.B., De Bonis, L., Coppens, C., Dejax, J., Denys, Ch.,  
533 Düringer, Ph., Eisenmann, V., Fanone, G., Fronty, P., Geraads, D., Lehmann, Th., Lihoreau,  
534 F., Louchart, A., Mahamat, A., Merceron, G., Mouchelin, G., Otero, O., Pelaez Campomanes,  
535 P., Ponce De Leon, M., Rage, J.C., Sapanet, M., Schuster, M., Sudre, J., Tassy, P., Valentin,  
536 X., Vignaud, P., Viriot, L., Zazzo, A., Zollikofer, Ch., 2002. A new hominid from the  
537 Miocene of Chad, central Africa. *Nature* 418, 145–151.
- 538
- 539 Brunet, M., Guy, F., Pilbeam, D., Lieberman, D.E., Likius, A., Mackaye, H.T., Ponce de  
540 Léon, M.S., Zollikofer, C.P.E., Vignaud, P., 2005. New material of the earliest hominid from  
541 the Upper Miocene of Chad. *Nature* 434, 752-755.
- 542
- 543 Buol, S.W., Southard, R.J., Graham, R.C., McDaniel, P.A., 2011. Vertisols: Shrinking and  
544 Swelling Dark Clay Soils. In: *Soil Genesis and Classification*, 6th Edition. Wiley-Blackwell,  
545 Hoboken, New Jersey, USA, pp. 385-396
- 546
- 547 Burke, K., 1976. The Chad Basin: an active intra-continental basin. *Tectonophysics* 36, 197-  
548 206.
- 549
- 550 Carignan, J., Hild, P., Mevelle, G., Morel, J., Yeghicheyan, D., 2001. Routine analyses of  
551 trace elements in geological samples using flow injection and low pressure on-line liquid  
552 chromatography coupled to ICP-MS: a study of reference materials BR, DR-N, UB-N, AN-G  
553 and GH. *Geostandards and Geoanalytical Research* 25, 187-198.

- 554  
555 Carmouze, J.P., 1976. La régulation hydrogéochemique du lac Tchad. Travaux et documents  
556 de l'ORSTOM n°58, 413 p.  
557
- 558 Contoux, C., Jost, A., Ramstein, G., Sepulchre, P., Krinner, G., Schuster, M., 2013. Megalake  
559 Chad impact on climate and vegetation during the late Pliocene and the mid- Holocene.  
560 *Climate of the Past* 9, 1417–1430.  
561
- 562 deMaster, D. J., 2003. The Diagenesis of Biogenic Silica: Chemical Transformations  
563 Occurring in the Water Column, Seabed, and Crust. In: H. D. Holland and K.Turekian (Eds)  
564 *Treatise on Geochemistry*, Elsevier, Pergamon Press, Oxford, pp. 87-98  
565
- 566 deMenocal, P.B., 2004. African climate change and faunal evolution during the Pliocene  
567 Pleistocene. *Earth Planetary Sciences* 220, 3–24.  
568
- 569 Düringer, Ph., Schuster, M., Genise, J.F., Likies A., Mackaye, H.T., Vignaud, P., Brunet, M.,  
570 2006. The first fossil fungus gardens of Isoptera: oldest evidence of symbiotic termite  
571 fungiculture (Miocene, Chad basin). *Naturwissenschaften* 93, 610-615.  
572
- 573 Feakins, S.J., deMenocal, P.B., 2010. Global and African regional climate during the  
574 Cenozoic. In: Werdelin, L., Sanders, W. (Eds.), *Cenozoic Mammals of Africa*. University of  
575 California Press.  
576
- 577 Gac, J.Y., 1980. Géochimie du bassin du lac Tchad. Bilan d'altération, de l'érosion et de la  
578 sédimentation. Documents de l'ORSTOM n°123, 251 p.  
579
- 580 Gac, J.Y., Droubi, A., Fritz, B., Tardy, Y., 1977. Geochemical behaviour of silica and  
581 magnesium during the evaporation of waters in Chad. *Chemical Geology* 19, 215-228.  
582
- 583 Genik, G.J., 1992. Regional framework, structural and petroleum aspects of rift basins in  
584 Niger, Chad and the Central African Republic (C.A.R.). *Tectonophysics* 213, 169-185.  
585
- 586 Güzel, N, Wilson, M.J., 1981. Clay-mineral studies of a soil chronosequence in southern  
587 Turkey. *Geoderma* 25, 113-129.LAY

- 588  
589 Jacques, L., 2007. Les préférences écologiques (paléorégimes alimentaires, paléohabitats) des  
590 grands mammifères herbivores des sites à hominidés du miocène supérieur du Nord Tchad.  
591 Reconstitution au moyen de l'analyse isotopique en carbone et oxygène du carbonate de  
592 l'émail dentaire, PhD Thesis. Université de Poitiers, np.-MI
- 593 NERAL STUDIES OF A SOIL CHRONOSE
- 594 Kusnir, I., Moutaye, H.A., 1997. Ressources minérales du Tchad : une revue. Journal of  
595 African Earth Sciences 24, 549-562.
- 596
- 597 Lebatard, A. E., Bourlès, D., Braucher, R., Arnold M., Durringer, Ph., Jolivet, M., Moussa, A.,  
598 Deschamps, P., Schuster, M., Roquin, C., Carcaillet, J., Lihoreau, F., Likius, A., Mackaye,  
599 H.T., Vignaud, P., Brunet, M., 2010. Application of the authigenic  $^{10}\text{Be}/^9\text{Be}$  dating method to  
600 continental sediments: Reconstruction of the Mio-Pleistocene sedimentary sequence in the  
601 early hominid fossiliferous areas of the northern Chad Basin. Earth and Planetary Science  
602 Letters 297, 57-70.
- 603
- 604 Leblanc, M., Favreau, G., Maley, J., Nazoumou, Y., Leduc, C., Stagnitti, F., van Oevelen,  
605 P.J., Delclaux, F., Lemoalle, J., 2006. Reconstruction of Megalake Chad using Shuttle Radar  
606 Topographic Mission data. Palaeogeography, Palaeoclimatology, Palaeoecology 239, 16-27.
- 607
- 608 Lee-Thorp, J., Likius, A., Mackaye, H.T., Vignaud, P., Sponheimer, M., Brunet, M., 2012.  
609 Isotopic evidence for an early shift to  $\text{C}_4$  resources by Pliocene hominins in Chad.  
610 Proceedings of the National Academy of Sciences 109, 20369-20372.
- 611
- 612 LeFur, S., Fara, E., Mackaye, H.T., Vignaud, P., Brunet, M., 2009. The mammal assemblage  
613 of the hominid site TM266 (Late Miocene, Chad Basin): ecological structure and  
614 paleoenvironmental implications. Naturwissenschaften 96, 565-574.
- 615
- 616 LeFur, S., Fara, E., Mackaye, H.T., Vignaud, P., Brunet, M., 2014. Toros-Menalla (Chad, 7  
617 Ma), the earliest hominin-bearing area: How many mammal paleocommunities? Journal of  
618 Human Evolution 69, 79-90.
- 619
- 620 Lemoalle, J., 1978. Relations silice-diatomées dans le Lac Tchad. Cahiers de l'ORSTOM,  
621 série Hydrobiologie vol. XII, n°2, 137-141.

- 622  
623 Leroy, S., Dupont, L., 1994. Development of vegetation and continental aridity in  
624 northwestern Africa during the Late Pliocene: the pollen record of ODP site 658.  
625 *Palaeogeography, Palaeoclimatology, Palaeoecology* 109, 295–316.  
626
- 627 Leroy, S., Dupont, L., 1997. Marine palynology of the ODP site 658 (N-W Africa) and its  
628 contribution to the stratigraphy of the Late Pliocene. *Geobios* 30, 351–359.  
629
- 630 Levin, N.E., 2015. Environment and Climate of Early Human Evolution. *Annual Review of*  
631 *Earth and Planetary Sciences* 43, 405-429.  
632
- 633 McLennan, S.M., 1989. Rare earth elements in sedimentary rocks: influence of provenance  
634 and sedimentary processes. In: B. R. Lipin & G.A. McKay (Eds.), *Geochemistry and*  
635 *Mineralogy of Rare Earth Elements, Reviews in Mineralogy*, 21, Mineral. Soc. of America,  
636 pp. 169-200  
637
- 638 Maley, J., 1972. La sédimentation pollinique actuelle dans la zone du lac Tchad (Afrique  
639 Centrale). *Pollen et Spores* 14, 263-307  
640
- 641 Maley, J. 1981. Etudes palynologiques dans le bassin du Tchad et paléoclimatologie de  
642 l'Afrique nord-tropicale de 30.000 ans à l'époque actuelle. *Travaux & Documents ORSTOM*,  
643 n° 129, 586 p.  
644
- 645 Maley, J., 2010. Climate and Palaeoenvironment evolution in north tropical Africa from the  
646 end of the Tertiary to the Upper Quaternary. *Palaeoecology of Africa* 30: 227-278.  
647
- 648 Maley, J. and Vernet, R., 2015. Populations and climatic evolution in north tropical Africa  
649 from the end of the Neolithic to the dawn of the modern era. *African Archaeological Review*  
650 32 (2), 179-232.  
651
- 652 Math, S.K., Murphy, S.P., 1994. Occurrence of iron rich high charge beidellite in vertisols of  
653 the Deccan plateau of India. *Applied Clay Science* 9, 303-316.  
654



- 655 Mestdagh, M.M., Vielvove L., Herbillon, A.J., 1980. Iron in kaolinite: II The relationship  
656 between kaolinite cristallinity and iron content. *Clay Mineralogy* 15, 1-12.  
657
- 658 Moussa, A., 2010. Les séries sédimentaires fluviales, lacustres et éoliennes du bassin du  
659 Tchad depuis le Miocène terminal, PhD thesis, Université de Strasbourg, 250 p.  
660
- 661 Moussa, A., Moussa, I., Abderamane, H., Schuster, M., Mackaye, H.T., Likius, A., Ahounta,  
662 D., Durringer, P., Vignaud, P., 2013. Synthèse géologique des dépôts sédimentaires  
663 continentaux d'âge Miocène et Pliocène du bassin du Tchad : proposition de nouvelles coupes  
664 géologiques à travers le bassin. *Revue Scientifique du Tchad*, n° Déc. 22-33.  
665
- 666 Novello, A., Lebatard, A.E., Moussa, A., Barboni, D., Sylvestre, F., Bourlès D.L., Paillès C.,  
667 Buchet, G., Decarreau, A., Durringer, P., Ghienne, J.F., Maley, J., Mazur, J.-C., Roquin, C.,  
668 Schuster, M., Vignaud, P., 2015a. Micro-biological remains investigations on a new  $^{10}\text{Be}/^9\text{Be}$   
669 dated lacustrine record from Chad: insight on the Miocene-Pliocene paleoenvironmental  
670 changes in Central Africa. *Palaeogeography, Palaeoclimatology, Palaeoecology* 430, 85-103.  
671
- 672 Novello, A., Lebatard, A.E., Moussa, A., Barboni, D., Sylvestre, F., Bourlès D.L., Paillès C.,  
673 Buchet, G., Decarreau, A., Durringer, P., Ghienne, J.F., Maley, J., Mazur, J.-C., Roquin, C.,  
674 Schuster, M., Vignaud, P., 2015b. Corrigendum to "Diatom, phytolith, and pollen records  
675 from a  $^{10}\text{Be}/^9\text{Be}$  dated lacustrine succession in the Chad basin: Insight on the Miocene  
676 Pliocene paleoenvironmental changes in Central Africa" [PALAEO: 430 (2015) 85–  
677 103]. *Palaeogeography, Palaeoclimatology, Palaeoecology*, 2016, vol. 442, p. 128  
678
- 679 Olivry, J.C., Chouret, A., Lemoalle, J., Bricquet, J.P., 1996. Hydrologie du lac Tchad.  
680 ORSTOM, Paris, 266 p.  
681
- 682 Otero, O., Pinton, A., Mackaye, H.T., Likius, A., Vignaud, P., Brunet, M., 2010. The fish  
683 assemblage associated with the late Miocene Chadian hominid (Toros-Menalla, Western  
684 Djurab) and its palaeoenvironmental significance. *Palaeontographica, Abt. a: Palaeozoology,*  
685 *Stratigraphy* 292, 21-51.  
686
- 687 Özkan, A.I., Ross, G.J., 1979. Ferruginous beidellites in Turkish soils. *Soil Science Society of*  
688 *America Journal* 43, 1242-1248.

- 689  
690 Pagani, M., Liu, Z., LaRiviere, J., Ravelo, A.C., 2010. High Earth-system climate sensitivity  
691 determined from Pliocene carbon dioxide concentrations. *Nature Geosciences* 3, 27–30.  
692
- 693 Paquet, H., 1967. Les montmorillonites des vertisols. Altération alcaline en milieu tropical.  
694 *Bulletin du Service de la Carte géologique d'Alsace et de Lorraine* 20, 293-306.  
695
- 696 Paquet, H., 1970. Evolution géochimique des minéraux argileux dans les altérations et les sols  
697 des climats méditerranéens et tropicaux à saisons contrastées. *Mémoire du Service de la Carte*  
698 *géologique d'Alsace et de Lorraine* 30, 212 p.  
699
- 700 Pédro, G., Carmouze, J.P., Velde, B., 1978. Peloidal nontronite formation in recent sediments  
701 of lake Chad. *Chemical Geology* 23, 139-149.  
702
- 703 Pinton, A., Otero, O., Likius, A., Mackaye, H.T., Vignaud, P., Brunet, M., 2010. Giants in a  
704 minute catfish genus: first description of fossil *Mochokus* (Siluriformes, Mochokidae) in the  
705 Late Miocene of Chad, including *M. Gigas*, sp. nov. *Journal of Vertebrate Paleontology* 31,  
706 22-31.  
707
- 708 Righi, D., Terribile, F., Petit, S. 1998. Pedogenetic formation of high-charge beidellite in a  
709 vertisol of Sardinia (Italy). *Clays and Clay Minerals* 46, 167-177. *Clays*  
710
- 711 Salzmann, U., Haywood, A.M., Lunt, D.J., Valdes, P.J., Hill, D.J., 2008. A new global biome  
712 reconstruction and data-model comparison for the Middle Pliocene. *Global Ecology and*  
713 *Biogeography* 17, 432–447.  
714
- 715 Salzmann, U., Williams, M., Haywood, A.M., Johnson, A.L.A., Kender, S., Zalasiewicz, J.,  
716 2011. Climate and environment of a Pliocene warm world. *Palaeogeography,*  
717 *Palaeoclimatology, Palaeoecology* 309, 1–8. **FORMATION OF HIGH-CHARGE**  
718 **BEIDELLITE IN A**
- 719 Sebag, D., Verrecchia, E.P., Lee, S.J., Durand, A., 2001. The natural hydrous sodium silicates  
720 from the northern bank of Lake Chad: occurrence, petrology and genesis. *Sedimentary*  
721 *Geology* 139, 15-31.  
722

- 723 Servant-Vildary, S., 1978. Etude des diatomées et paléolimnologie du Bassin tchadien au  
724 Cénozoïque supérieur. Travaux et Documents de l'ORSTOM, n°82, 2 tomes, Paris, 346 p.  
725
- 726 Servant, M., 1983. Séquences continentales et variations climatiques : évolution du bassin du  
727 Tchad au Cénozoïque supérieur. Travaux et Documents de l'ORSTOM 159, 573 p.  
728
- 729 Schuster, M., 2002. Sédimentologie et paléoécologie des séries à vertébrés du paléolac Tchad  
730 depuis le Miocène supérieur. PhD thesis, Université de Strasbourg, 152 p.  
731
- 732 Schuster, M., Roquin, C., Durringer, Ph., Brunet, M., Fontugne, M., Mackaye, H.T.,  
733 Vignaud, P., Ghienne, J.-F., 2005. Highlighting Holocene Lake Mega-Chad paleoshorelines  
734 from space. Quaternary Science Reviews 24, 1821-1827.  
735
- 736 Schuster, M., Durringer, P., Ghienne, J.-F., Vignaud, P., Mackaye, H.T., Likius, A., Brunet,  
737 M., 2006. The age of the Sahara Desert. Science 311, 821.  
738
- 739 Schuster, M., Durringer, Ph., Ghienne, J.-F., Roquin, C., Sepulchre, P., Moussa, A., Lebatard,  
740 A.-E., Mackaye, H.T., Likius, A., Vignaud, P., Brunet M., 2009. Chad Basin:  
741 paleoenvironments of the Sahara since the late Miocene. Comptes Rendus Geosciences 341,  
742 612-620.  
743
- 744 Schneider, J.L., Wolff, J.P., 1992. Carte géologique et Cartes hydrologiques à 1/1,500,000 de  
745 la République du Tchad – Mémoire explicatif. Documents du Bureau des Recherches  
746 Géologiques et Minières n° 209, vol.1, np.  
747
- 748 Schneider, J.L., 1989. Géologie et hydrologie du Tchad. PhD thesis, Université d'Avignon,  
749 271 p.  
750
- 751 Sepulchre, P., Ramstein, G., Fluteau, F., Schuster, M., Tiercelin, J.-J., Brunet, M., 2006.  
752 Tectonic Uplift and Eastern Africa Aridification 313, 1419-1423.  
753
- 754 Stoffregen, R.E., Alpers, C.N., Jambor, J.L., 2000. Alunite-jarosite crystallography,  
755 thermodynamics, and geochemistry. In: C.N. Alpers, J.L. Jambor, and D.K. Nordstrom (Eds),

756 Sulfate Minerals: Crystallography, Geochemistry, and Environmental Significance, Mineral.  
757 Society of America, Washington, D.C., pp. 453-480

758

759 Swezey, C.S., 2009. Cenozoic stratigraphy of the Sahara, Northern Africa. *Journal of African*  
760 *Earth Sciences* 53, 89–121.

761

762 UNEP, 2004. Global International Water Assessment. Regional Assessment 43, Lake Chad  
763 Basin. 154 p.

764

765 Vignaud, P., Durringer, P., Mackaye, H.T., Andossa, L., Blondel, C., Boisserie, J.R., De  
766 Bonis, L., Eisenmann, V., Géraads, D. Guy, F., Lehmann, T., Lihoreau, F., Lopez-Martinez,  
767 N., Mourer-Chauviré, C., Otero, O., Rage, J.-C., Schuster, M., Viriot, L., Zazzo, A., Brunet,  
768 M., 2002. Geology and Palaeontology of the Upper Miocene Toros-Menalla hominid locality,  
769 Chad. *Nature* 418, 152–155.

770

771 White, F., 1983. The Vegetation Map of Africa, *Recherches sur les ressources naturelles*.  
772 Office de la Recherche Scientifique et Technique Outre-Mer, United Nations Educational,  
773 Scientific and Cultural Organization, Paris, 384 p.

774

775 Wilson, M.J., 2013. Smectites Clay Minerals: Beidellite, In: Deer, Howie and Zussman (Eds.)  
776 *Rock-Forming Minerals vol 3C: Sheet silicates: Clay minerals*, The Geological Society,  
777 London, pp 257-277.

778

779 Wilson, M.J., Mitchell, B.D., 1979. A comparative study of vertisols and entisols from the  
780 Blue Nile plains of Sudan. *Egyptian Journal of Soil Science* 19, 207-220.

781

782 Zazzo, A., Bocherens, H., Brunet, M., Beauvilain, A., Billiou, D., Mackaye, H.T., Vignaud,  
783 P., Mariotti, A., 2000. Herbivore paleodiet and paleoenvironmental changes in Chad during  
784 the Pliocene using stable isotope ratios of tooth enamel carbonate. *Paleobiology* 26, 294-309.

785

## 786 **Figure captions**

787 **Figure 1:** Location map showing the Chad Basin, the modern Lake Chad (in blue), and the  
788 Holocene Lake Mega-Chad (broken line).

789 Black dot: Bol core location (13°27'N, 14°44'E). Red dots: Miocene-Pliocene fossiliferous  
790 areas of the Djurab desert: TM, Toros Menalla; KB, Kossom Bougoundi; KL, Kollé; KT,  
791 Koro Toro. Black squares: location of wells drilled in the Kanem region (from Schneider and  
792 Wolf, 1992; Swezey, 2009)

793

794 **Figure 2:** Bol core lithology. 2a: whole core lithology; 2b: detailed lithology for the sampled  
795 part of Bol core.

796 The depth (m), label, and  $^{10}\text{Be}/^9\text{Be}$  ages (Ma) of the samples selected for micro-biological  
797 (Novello et al., 2015a, 2015b) and mineralogy analyses (this study) are indicated on the  
798 figure. The stratigraphic position of these samples is marked on the sequence with red stars.  
799 KB, KL, KT and TM: as in Figure 1.

800

801 **Figure 3:** Typical powder XRD diagram (sample 32a).

802 Sm: smectite; K: kaolinite; I: illite; F: K-feldspar; Q: quartz; A: anatase; Op: opale.

803

804 **Figure 4:** Relative amounts of the main recurrent minerals resulting from the XRD analysis.  
805 From the left to the right: A: K-feldspar; B:  $\text{TiO}_2$ ; C: clays; D: quartz.

806

807 **Figure 5:** Relative amounts of clay minerals from XRD analysis.

808 Sm: smectite; K: kaolinite; I: illite.

809

810 **Figure 6:** Typical XRD patterns (sample 17h) of oriented aggregates (<2  $\mu\text{m}$  fraction).

811 a: air dry; b: after ethylene glycol saturation.

812

813 **Figure 7:** XRD pattern of sample 01d after hydrazine saturation.

814

815 **Figure 8:** Chondrite normalized diagrams of the clay fraction chemistry of the Bol samples.

816 a: REE pattern; b: extended trace elements pattern.

817

818 **Figure 9:** Sedimentation rates of the Bol core.

819

820 **Table captions**

821

822 **Table 1:** Amounts of disordered kaolinite from XRD patterns of clay samples after hydrazine  
823 saturation.

824

825 **Table 2:** Chemistry of the clay fractions (<2  $\mu\text{m}$  fraction).

826 °: chemistry of pellets in samples 21j and 35e.

827

828 **Table 3:** Local ( $\approx 10 \text{ nm}^2$ ) SEM-EDX chemistry of samples.

829

830 **Table 4:**  $\text{La}_\text{N}/\text{Yb}_\text{N}$  and  $\text{Eu}_\text{N}/\text{Eu}_\text{N}^{**}$  values of the Bol clay samples.

831 Suffix “N” denotes a chondrite normalized value.  $\text{Eu}_\text{N}/\text{Eu}_\text{N}^{**}$ :  $\text{Eu}_\text{N}/(\text{Sm}_\text{N}+\text{Gd}_\text{N})/2$ . °= values  
832 for pellets in samples 21j and 35e.

833

834 **Supplementary material**

835

836 **Table S1:** Location of the studied samples in the Bol core.

837 \*: selected samples for the detailed study of clay mineralogy; \*\*: samples dated and  
838 previously studied for micro-biological remains (Novello et al., 2015a, 2015b).

839

Table 1.

<b>Sample</b>	<b>Depth (m)</b>	<b>Disordered Kaolinite (%)</b>
1d	74.0	83
8n	105.0	59
13e	127.0	48
17h	147.0	45
21j	169.3	60
25a	203.0	62
27n	224.3	68
30j	251.0	50
32e	270.4	52
35e	297.2	65



Table 2.

Sample	SiO <sub>2</sub>	Al <sub>2</sub> O <sub>3</sub>	Fe <sub>2</sub> O <sub>3</sub>	MnO	MgO	CaO	Na <sub>2</sub> O	K <sub>2</sub> O	TiO <sub>2</sub>	P <sub>2</sub> O <sub>5</sub>	LI	Sum
1d	47.50	20.79	7.69	0.04	1.55	1.34	0.49	1.13	0.85	0.52	17.37	99.27
8n	51.76	18.71	7.52	0.06	1.35	1.21	0.39	1.55	0.85	0.44	16.49	100.31
13e	51.53	19.76	8.21	0.06	1.07	0.79	0.35	1.34	1.00	0.14	16.37	100.62
17h	48.82	19.73	8.24	0.09	1.41	1.01	0.28	1.40	0.80	0.29	16.67	98.74
21j	58.54	17.09	8.44	0.06	0.62	0.45	0.12	0.96	0.84	0.22	12.33	99.66
21j*	52.55	16.59	8.44	0.04	0.49	1.93	0.09	0.75	0.72	0.23	16.87	98.69
25a	53.75	18.53	7.17	0.08	0.95	0.97	0.30	1.41	0.88	0.26	14.87	99.17
27n	54.99	15.55	3.72	0.04	0.48	1.96	0.10	0.69	0.57	0.07	20.61	98.76
30j	46.91	19.02	9.00	0.06	0.84	2.41	0.08	1.13	0.85	0.29	18.19	98.78
32e	53.42	17.53	7.04	0.10	1.32	1.01	0.30	1.35	0.83	0.18	15.61	98.68
35e	48.95	14.69	8.26	0.05	0.48	3.32	0.08	0.70	0.67	0.19	21.58	98.97
35e *	60.81	16.32	7.66	0.05	0.67	0.56	0.11	0.95	0.76	0.14	12.10	100.11

Table 3.

Sample	01d	08n	12L	21e	27n	30a	34e
SiO <sub>2</sub>	60.7	59.6	57.4	63.8	63.0	55.6	59.4
TiO <sub>2</sub>	1.0	0.9	0.7	1.0	0.7	0.8	1.2
Al <sub>2</sub> O <sub>3</sub>	23.5	26.0	27.4	23.7	26.2	28.0	28.0
Fe <sub>2</sub> O <sub>3</sub>	8.7	9.4	10.6	6.8	6.8	11.3	8.2
MnO	0.1	0.0	0.1	0.1	0.1	0.1	0.0
MgO	3.1	1.3	1.3	1.6	1.2	1.4	1.1
CaO	0.8	0.9	0.9	0.8	0.5	0.8	0.7
Na <sub>2</sub> O	0.8	0.7	0.6	0.8	0.5	0.5	0.4
K <sub>2</sub> O	1.3	1.0	0.9	1.4	0.9	1.5	0.9

Table 4.

Sample	La <sub>N</sub> /Yb <sub>N</sub>	Eu <sub>N</sub> /Eu <sub>N</sub> **
1d	11.6	0.74
8n	13.9	0.66
13e	20.0	0.66
17h	15.2	0.66
21j *	12.1	0.64
21j	13.7	0.66
25a	13.0	0.66
27n	15.3	0.67
30j	13.8	0.65
32e	16.3	0.59
35e	12.7	0.62
35e *	14.6	0.59

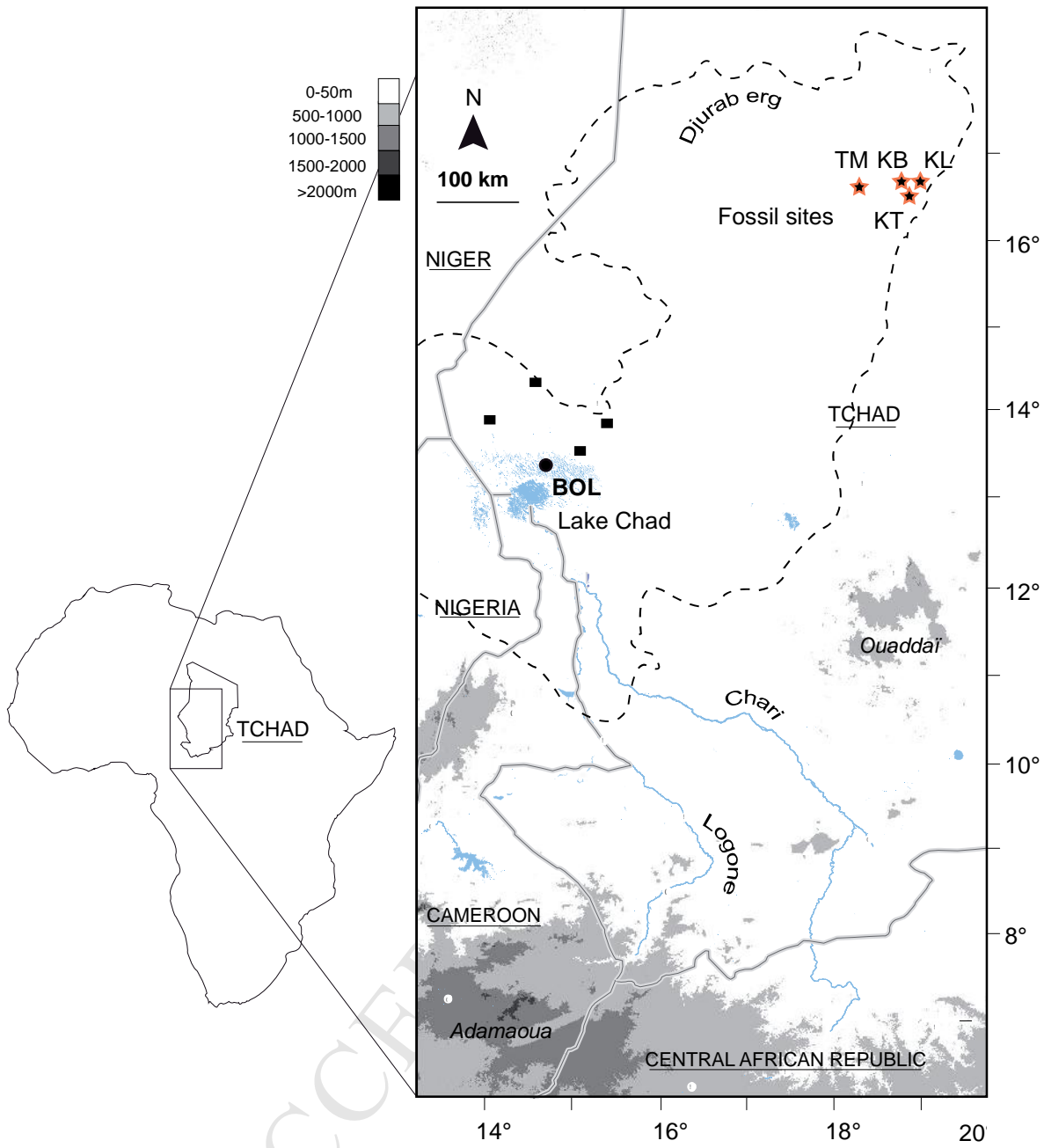


Fig. 1

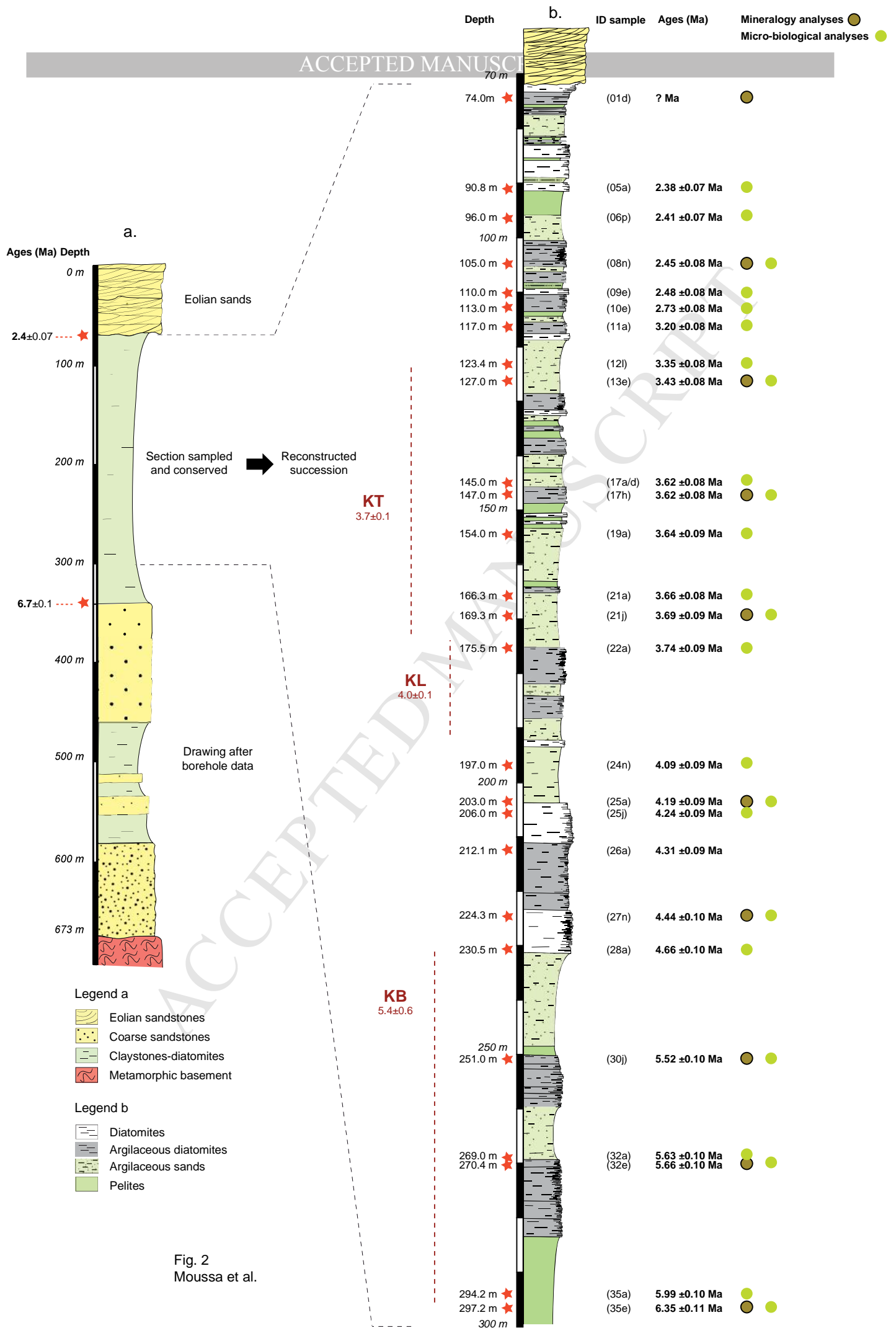
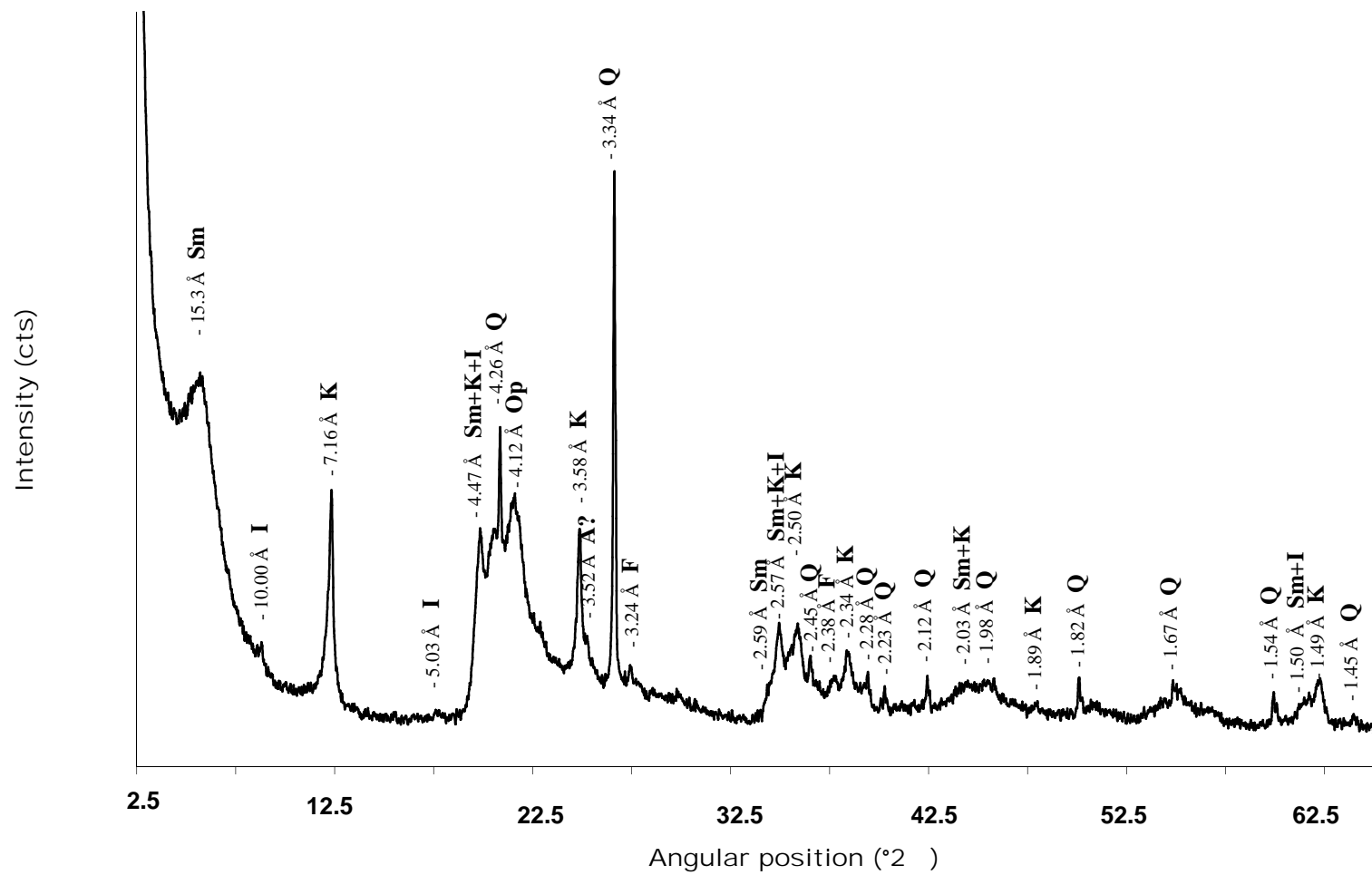
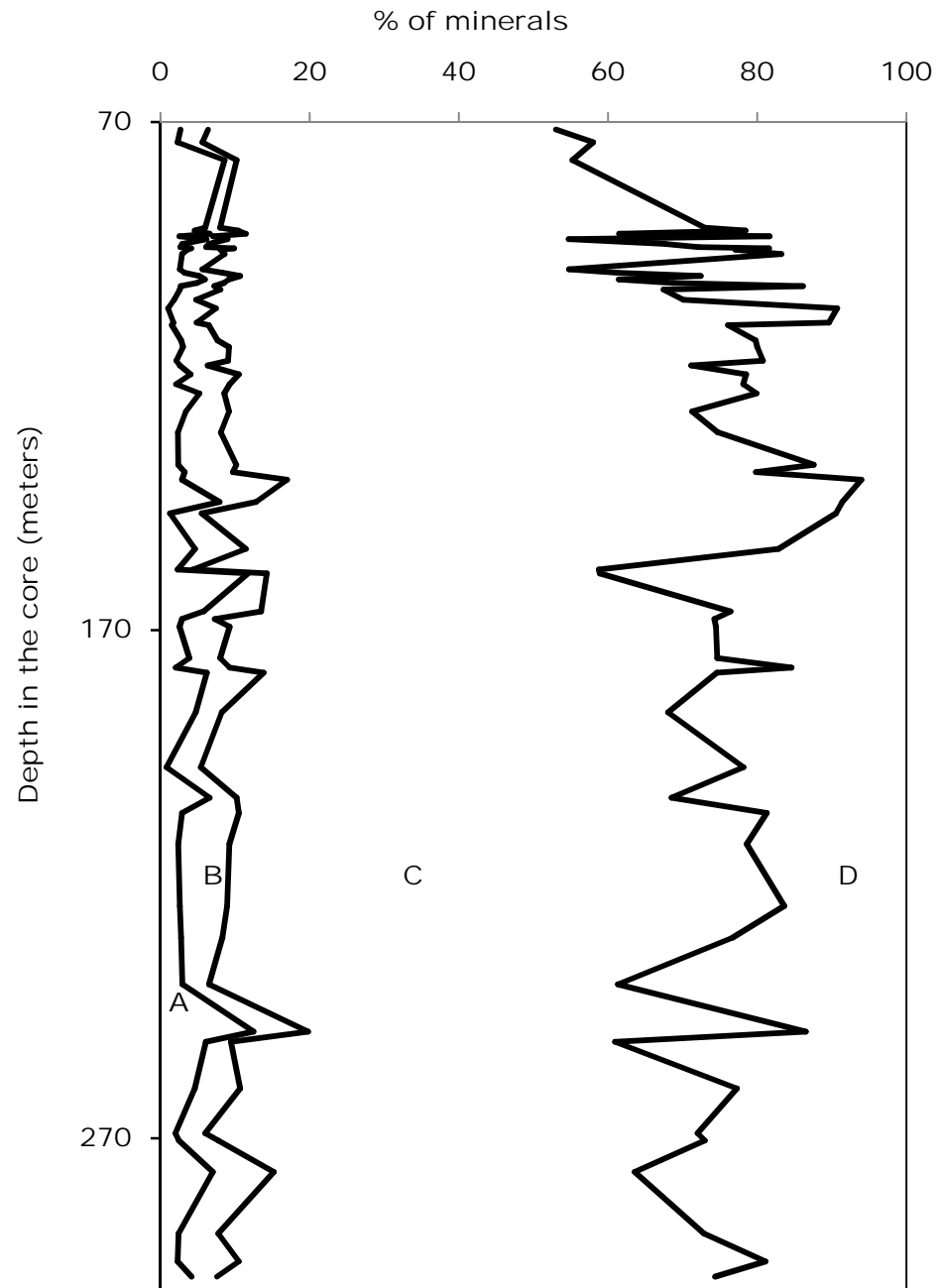


Fig. 2  
Moussa et al.



**Fig.3**  
Moussa et al.



**Fig.4**  
**Moussa et al.**



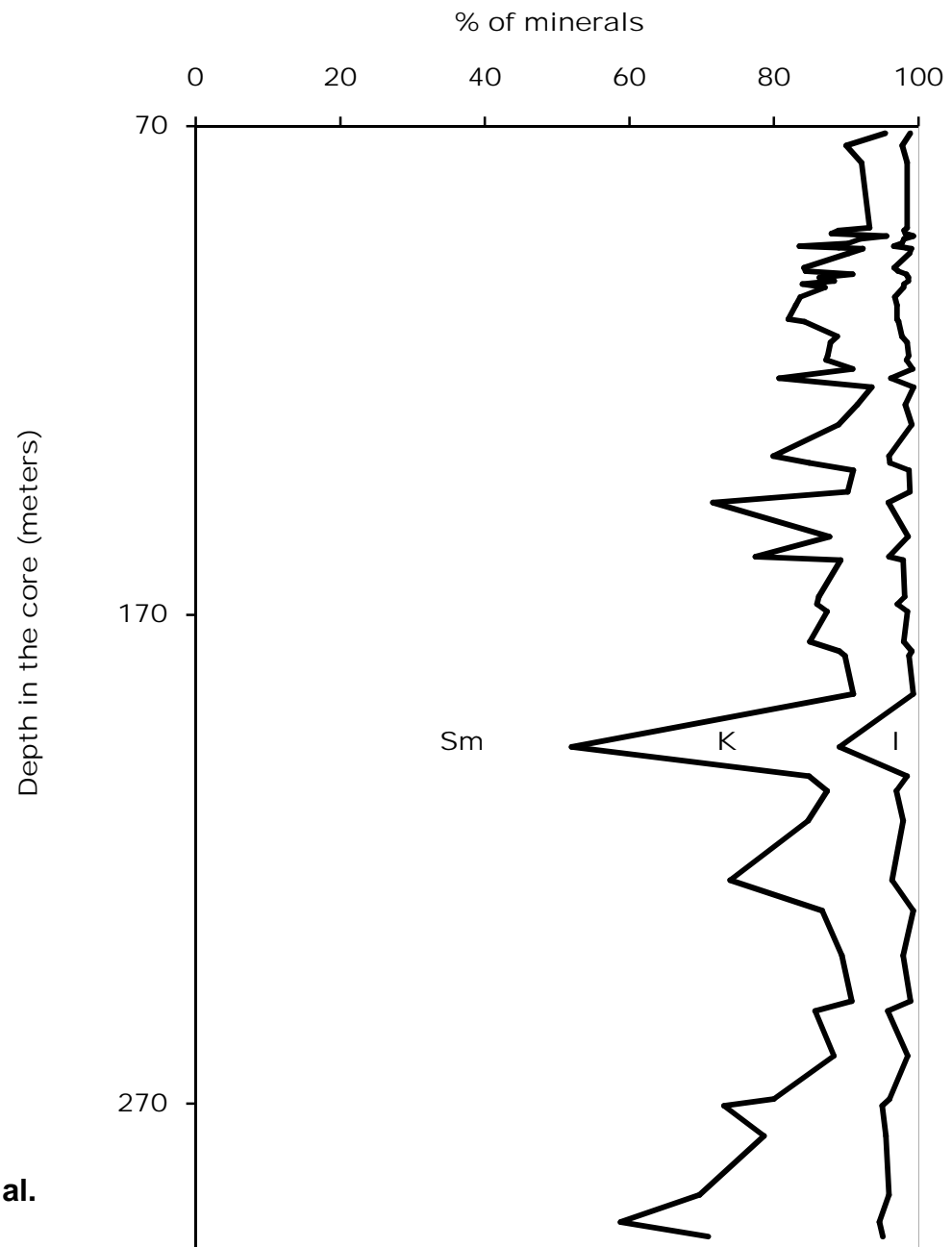


**Fig.5**  
**Moussa et al.**

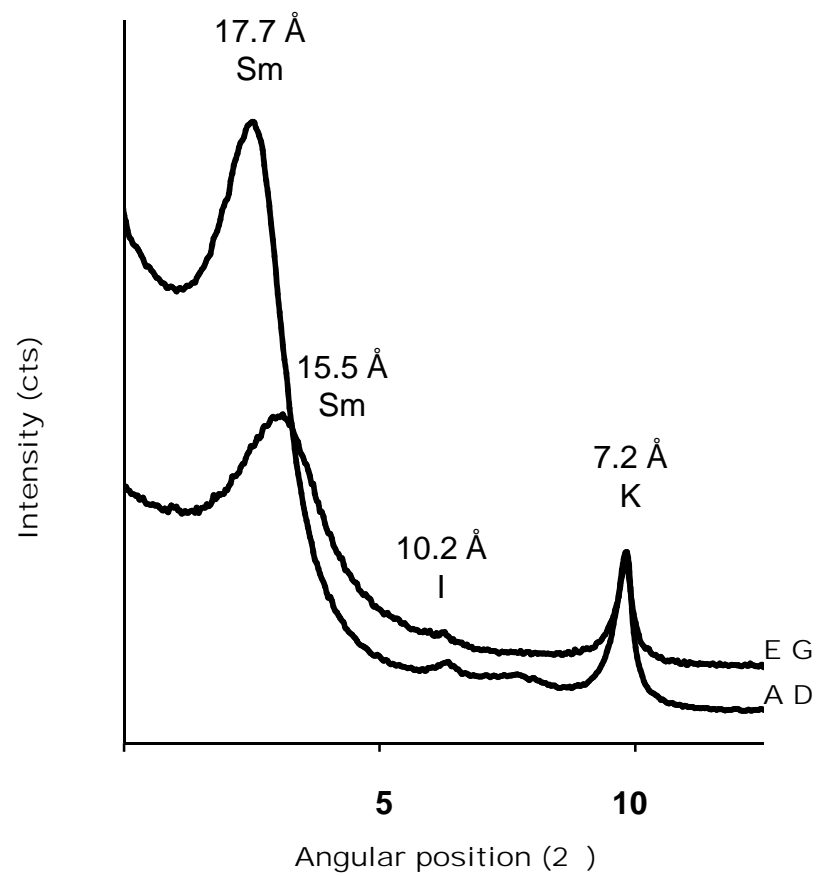


**Fig.6**  
**Moussa et al.**

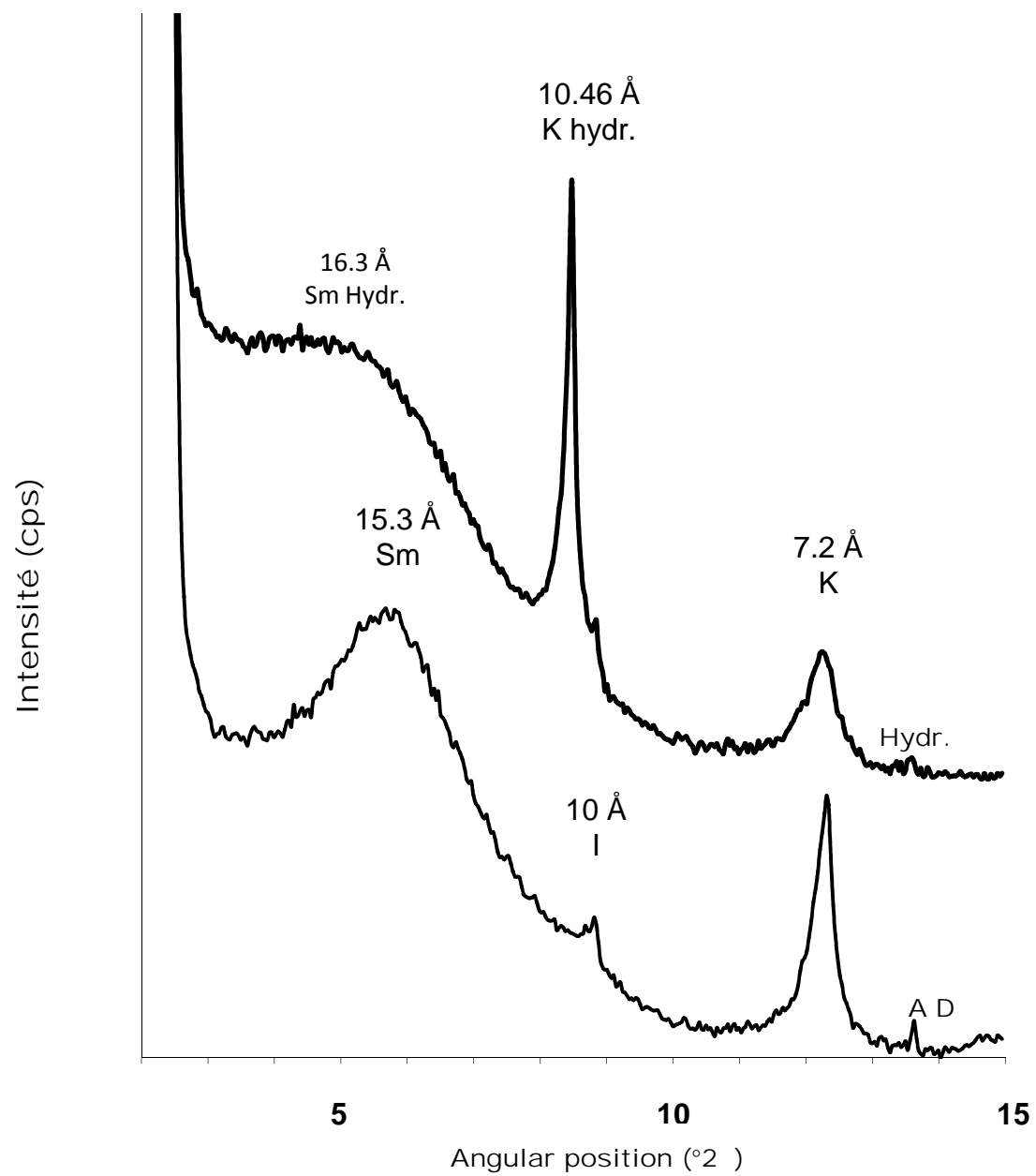


**Fig.7**  
**Moussa et al.**

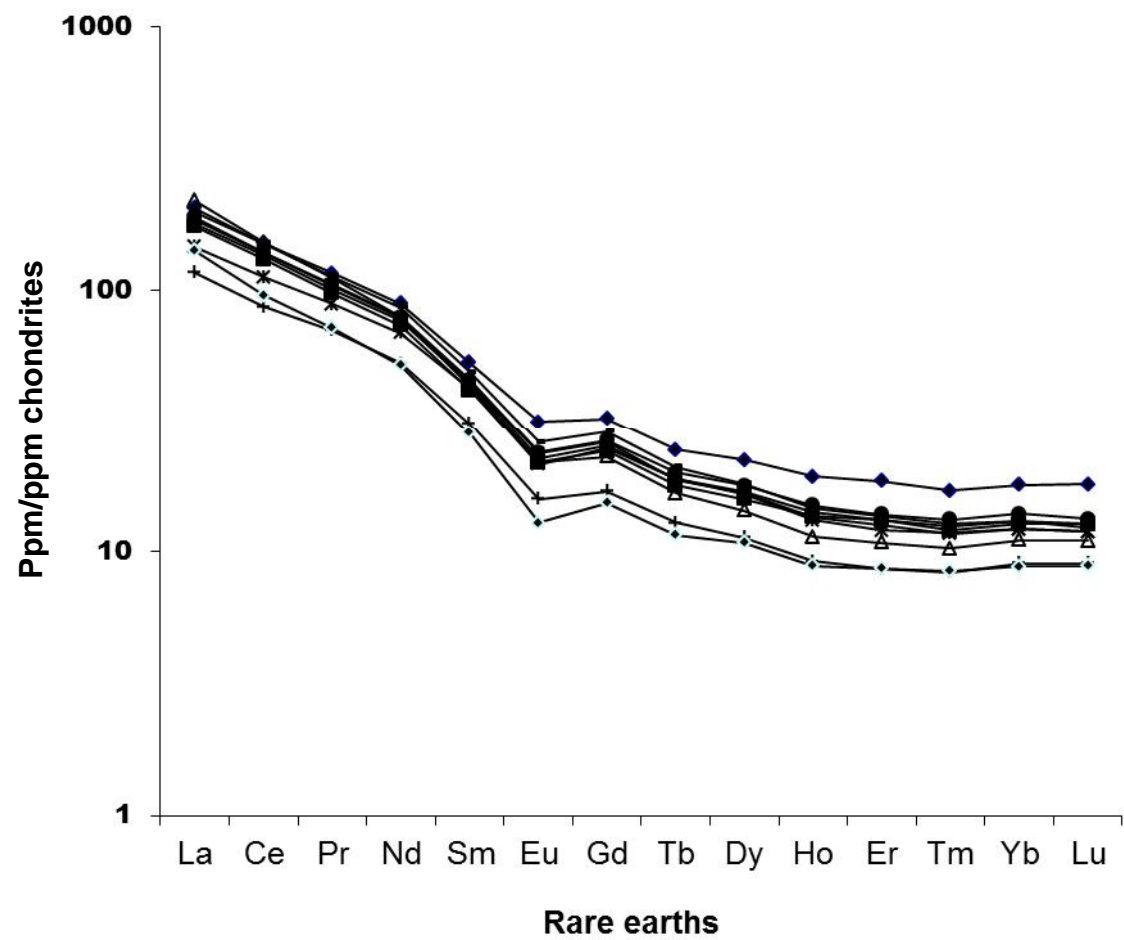
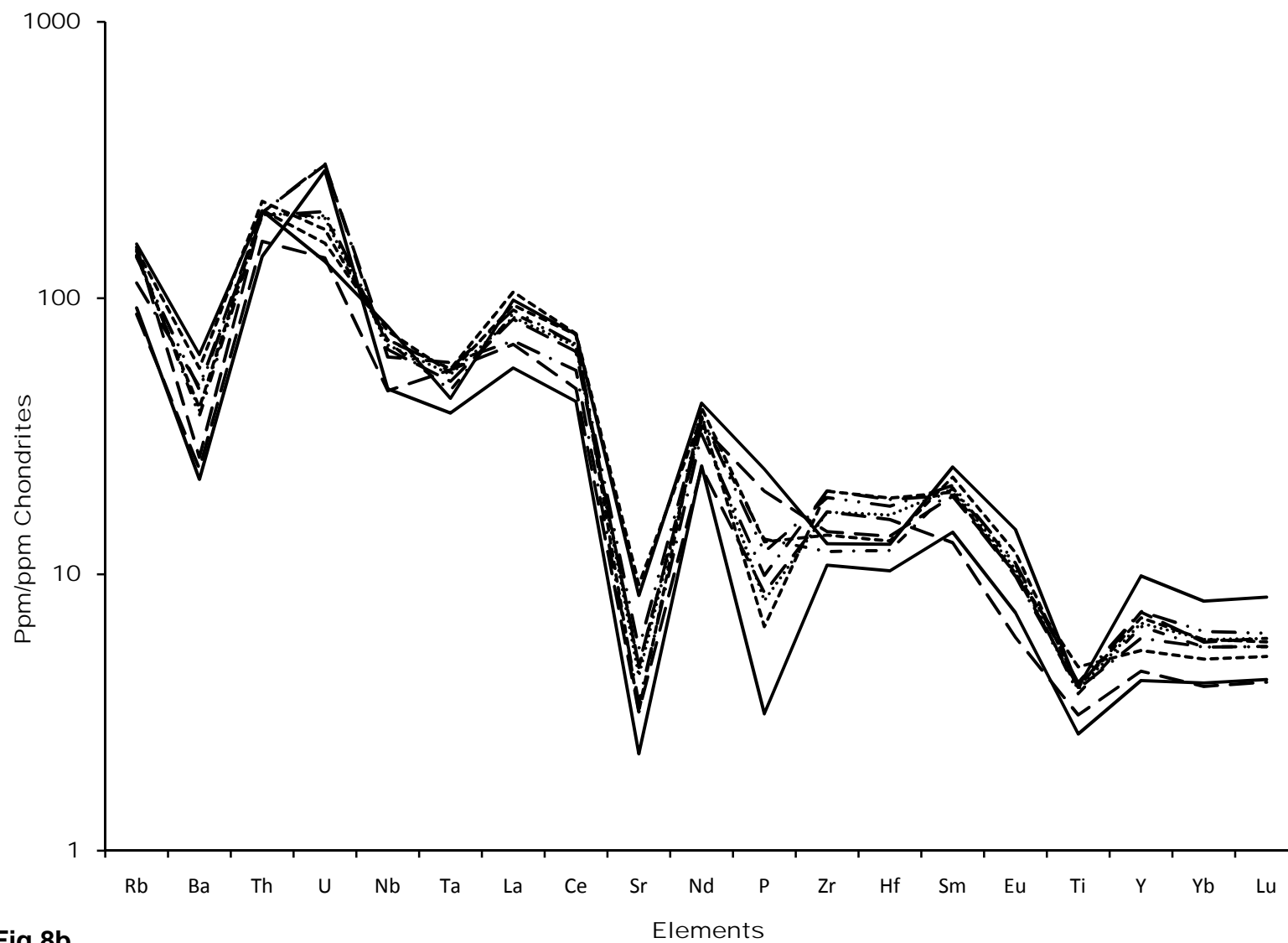
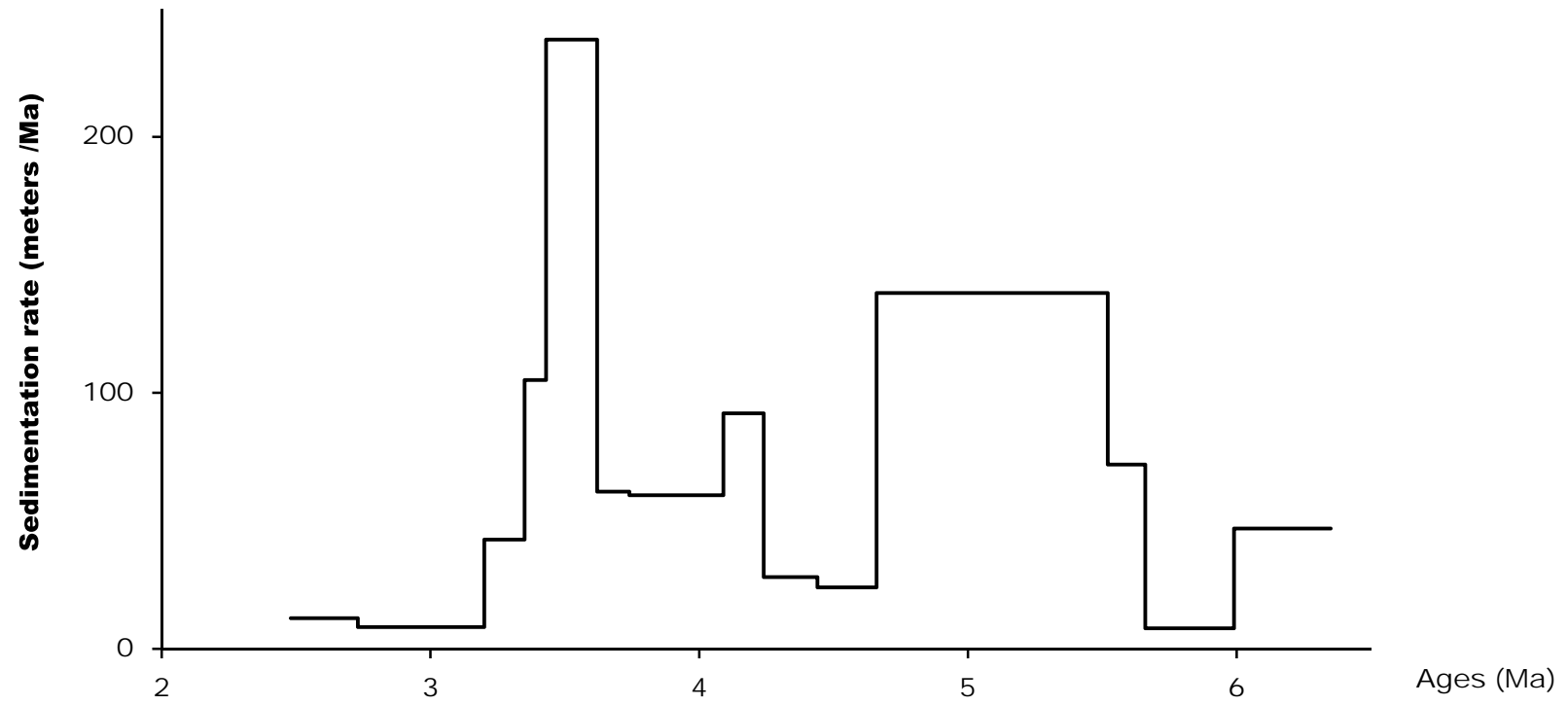


Fig.8a  
Moussa et al.



**Fig.8b**  
**Moussa et al.**



Moussa et al.  
Fig.9

**Highlights** (85 characters maximum by bullet, space included):

Sediments are dominated by detrital clays, more or less mixed with silt and diatomite;

These sediments point to a permanent (recurrent) lake(s) between 6.7-2.3 Ma at Bol;

The dominant clay is a Fe-beidellite, a feature of present-day vertisols;

Vertisols near Bol suggest a Sahelo-Sudanian-like climate between 6.7-2.3 Ma;

Changes in sedimentation rate suggest an alternating of wet and dry periods.